

Nucleon momentum distributions, their spin-isospin dependence, and short-range correlationsM. Alvioli,^{1,*} C. Ciofi degli Atti,² L. P. Kaptari,^{3,4,†} C. B. Mezzetti,^{2,5} and H. Morita⁶¹*ECT*, European Center for Theoretical Studies in Nuclear Physics and Related Areas, Strada delle Tabarelle 286, I-38123 Villazzano (TN), Italy*²*Istituto Nazionale di Fisica Nucleare, Sezione di Perugia, Via Alessandro Pascoli, I-06123, Italy*³*Department of Physics, University of Perugia and Istituto Nazionale di Fisica Nucleare, Sezione di Perugia, Via Alessandro Pascoli, I-06123, Italy*⁴*Bogoliubov Laboratory of Theoretical Physics, 141980, JINR, Dubna, Russia*⁵*Department of Chemistry and Industrial Chemistry, University of Pisa, Via Risorgimento 35, I-56126, Italy, and Consorzio Interuniversitario Nazionale per la Scienza e Tecnologia dei Materiali, Via Giuseppe Giusti 9, Pisa I-50121, Italy*⁶*Sapporo Gakuin University, Bunkyo-dai 11, Ebetsu 069-8555, Hokkaido, Japan*

(Received 2 November 2012; revised manuscript received 30 January 2013; published 5 March 2013)

The nucleon momentum distribution $n_A(k)$ for $A = 2, 3, 4, 16$, and 40 nuclei is systematically analyzed in terms of wave functions resulting from advanced solutions of the nonrelativistic Schrödinger equation, obtained within different many-body approaches based upon different realistic bare nucleon-nucleon (NN) interactions featuring similar short-range repulsion and tensor interactions. Particular attention is paid to the separation of the momentum distributions into the mean-field and short-range correlation (SRC) contributions. It is shown that although at high values of the momentum k different approaches lead to some quantitative differences, these do not hinder the general conclusion that the high-momentum behavior ($k \gtrsim 1.5\text{--}2 \text{ fm}^{-1}$) of all nuclei considered are very similar, exhibiting the well-known scaling behavior with the mass number A , independently of the used many-body approach and the details of the bare NN interaction. To analyze and understand the frequently addressed question concerning the relationships between the nucleus, $n_A(k)$, and the deuteron, $n_D(k)$, momentum distributions, the spin (S)-isospin (T) structure of few-nucleon systems and complex nuclei is analyzed in terms of realistic NN interactions and many-body approaches. To this end, the number of NN pairs in a given (ST) state, viz., (ST) = (10), (00), (01), and (11), and the contribution of these states to the nucleon momentum distributions are calculated. It is shown that, apart from the (00) state, which has very small effects, all other spin-isospin states contribute to the momentum distribution in a wide range of momenta. It is shown that for all nuclei considered the momentum distributions in the states $T = 0$ and $T = 1$ exhibit at $k \gtrsim 1.5\text{--}2 \text{ fm}^{-1}$ very similar behaviors, which represents strong evidence of the A -independent character of SRCs. The ratio $n_A(k)/n_D(k)$ is analyzed in detail, stressing that in the SRC region it always increases with the momentum and the origin of such an increase is discussed and elucidated. The relationships between the one- and two-body momentum distributions, considered in a previous paper, are discussed and clarified, pointing out the relevant role played by the center-of-mass motion of a correlated pair in the (10) state. Eventually, the values of the the probability of high-momentum components in nuclei and the per nucleon probability a_2 of deuteronlike configurations in nuclei are calculated, and the relationship of the present approach with the many-body methods based upon low-momentum effective interactions is briefly discussed.

DOI: [10.1103/PhysRevC.87.034603](https://doi.org/10.1103/PhysRevC.87.034603)

PACS number(s): 21.30.Fe, 21.60.-n, 24.10.Cn, 25.30.-c

I. INTRODUCTION

Recent experiments on two-nucleon knockout reactions at high values of the four-momentum transfer on carbon using protons, $A(p, ppN)X$ [1], and electrons, $A(e, e'pN)X$ [2], as well as experiments on inclusive quasielastic (q.e.) electron scattering $A(e, e')X$ [3–5], have provided robust evidence on the long-hunted ground-state nucleon-nucleon (NN) short-range correlations (SRCs), demonstrating that in both types of processes the projectile had interacted with a nucleon belonging to a correlated NN pair [6].

In exclusive experiments, where the knowledge of both the three-momentum transfer \mathbf{q} and the momentum of a fast detected proton \mathbf{p} allows one to reconstruct the momentum $\mathbf{k}_1 = \mathbf{p} - \mathbf{q} \equiv -\mathbf{p}_{\text{miss}}$ that the struck proton had before the interaction [provided the final-state interaction (FSI) could be disregarded], it has been found [1] that in the region $1.4 < |\mathbf{p}_{\text{miss}}| < 2.8 \text{ fm}^{-1}$ the removal of a proton was almost always accompanied by the emission of a nucleon N (mostly a neutron) carrying a momentum roughly equal to $-\mathbf{k}_1$. At the same time, in the q.e. inclusive experiment $A(e, e')X$, the ratio of the cross section off a nucleus A to the cross section off the deuteron or ${}^3\text{He}$ in the region of the Bjorken scaling variable $1.5 \lesssim x_{Bj} \lesssim 2$ (the region of x_{Bj} where q.e. scattering off a correlated NN pair is expected to occur), exhibits a constant behavior, indicating that, in agreement with theoretical predictions [7], the virtual photon interacted with a nucleon of a correlated NN pair. The exclusive experiment,

*Present address: CNR-IRPI, Istituto di Ricerca per la Protezione Idrogeologica, Via Madonna Alta 126, I-06128 Perugia, Italy.

†Supported through the program “Rientro dei Cervelli” of the Italian Ministry of University and Research.

moreover, provided evidence not only on SRCs in general, but also, in particular, of the dominance of proton-neutron (pn) deuteronlike tensor correlations occurring in states (ST) = (10), where spin is given as (S) and isospin as (T), as predicted by several realistic calculations [8–11]; the experimental data [1] have also provided information on the center-of-mass (c.m.) momentum distribution of the correlated NN pair, finding agreement with predictions made long ago [12].

Recent reviews on experiments providing information on SRCs and their theoretical interpretations can be found in Refs. [13,14]. A detailed picture of SRC is, however, still limited to the ^{12}C nucleus, so that extension to other nuclei is necessary to have a general quantitative picture of SRC through the periodic table. In a systematic study of SRC, particular attention should be given to the experimental and theoretical investigations of: (i) the relative and c.m. momentum dependencies of SRC, (ii) their spin-isospin structure, (iii) the relative role of two-nucleon ($2N$) and three-nucleon ($3N$) correlations. We discuss $3N$ SRCs in a separate paper; here we concentrate on $2N$ SRCs.

In configuration space these can be defined as those deviations from the independent motion of two nucleons, moving in a mean field, when they approach relative distances $r_{12} = |\mathbf{r}_1 - \mathbf{r}_2| \equiv r \lesssim 1.2\text{--}1.5$ fm; according to theoretical calculations, in this region, owing to the very nature of the NN interaction [in particular to its central short-range repulsion and the tensor attraction in (ST) = (10) state], the two-body mean-field density is strongly suppressed and $2N$ correlated motion dominates. The details of $2N$ SRC depend upon the spin-isospin state of the correlated NN pair, as well as upon the region of the nucleus one is considering, i.e., upon the c.m. motion of the pair $\mathbf{R} = (\mathbf{r}_1 + \mathbf{r}_2)/2$. To investigate these details, one has to take advantage of the high-momentum components generated by SRCs that lead to peculiar configurations of the nuclear wave function in momentum space [7]. As a matter of fact, if nucleons “1” and “2” become strongly correlated at short distances, the momentum configurations, in the nucleus c.m. frame, are characterized by $\mathbf{k}_2 \simeq -\mathbf{k}_1$, $\mathbf{k}_{A-2} = \sum_{i=3}^A \mathbf{k}_i \simeq 0$, and not by the mean-field configuration $\sum_{i=2}^A \mathbf{k}_i \simeq -\mathbf{k}_1$, i.e., when the high momentum nucleon is balanced by the entire $A - 1$ nucleons, each of them carrying an average momentum of the order $\simeq \mathbf{k}/(A - 1)$. Thus, if a correlated nucleon with momentum \mathbf{k}_1 acquires a momentum \mathbf{q} from an external probe, and is removed from the nucleus and detected with momentum $\mathbf{p} = \mathbf{k}_1 + \mathbf{q}$, the partner nucleon should be emitted with momentum $\mathbf{k}_2 \simeq -\mathbf{k}_1 = \mathbf{q} - \mathbf{p} = \mathbf{p}_{\text{miss}}$.

Such a qualitative picture is, however, strictly valid only if the c.m. momentum of the correlated pair was zero before nucleon removal and, moreover, if the two correlated nucleons leave the nucleus without interacting between themselves and with the nucleus ($A - 2$). These effects have to be carefully evaluated when attempting to extract the momentum distribution from experimental cross sections. Within a mean-field many-body approach, the main effect of SRCs is to deplete the occupancy of single-particle shell-model states and to make the occupation of levels above the Fermi sea different from zero; this leads to a decrease of the momentum distribution at values of $|\mathbf{k}|$ roughly less than the

Fermi momentum k_F and to an increase of it, by orders of magnitude, with respect to the mean-field distribution [15]. In this context, it has been pointed out that even a low-resolution measurement of the one-body momentum distribution at $|\mathbf{k}| \gtrsim 2\text{--}3$ fm $^{-1}$, where mean-field effects are negligible, may provide precious information on SRCs [16].

Though the most direct way to investigate SRCs would be via experiments that detect a pair of back-to-back nucleons in the final state, also experiments which are sensitive to the one-body momentum distributions could be very useful. We have analyzed two-nucleon momentum distributions in two previous papers [10,11]; here we concentrate on the one-nucleon momentum distribution $n_A(k)$, with the aim of clarifying some points concerning, particularly, its SRCs and spin-isospin structures. We quantitatively clarify to what extent the high-momentum part of $n_A(k)$ can be associated to the deuteron momentum distribution $n_D(k)$. To this end we show that such an association, which is only qualitatively correct, has been motivated either from the results of approximate many-body approaches [17–20], or from just assuming it as an input in pioneering Monte Carlo many-body calculations of $n_A(k)$ [21].

Recently, the momentum distributions of few-nucleon systems and complex nuclei have been calculated within sophisticated many-body approaches [10,11,22–34], using modern realistic interactions [35–39]. For this reason it seems to us appropriate to update the situation concerning the relationship between the momentum distributions of a nucleus A , where all $2N$ spin-isospin states may contribute, and the momentum distribution of the deuteron, where only the state (ST) = (10) is present.

Our paper is organized as follows. Our formalism, based upon proper spin-isospin dependent one- and two-body density matrices, which allows one to calculate the various spin-isospin components of the nucleon momentum distribution $n_A(k)$, is presented in Sec. II. In Sec. III we (i) provide some general definitions of the one- and two-body momentum distributions, (ii) illustrate the way SRCs influence the momentum distribution, (iii) critically analyze the way the probability of SRCs can be defined, and (iv) present a systematic comparison of the momentum distributions of $A = 2, 3, 4, 16$, and 40 , nuclei resulting from different many-body calculations and NN interactions. The values of the calculated number of pairs in different spin-isospin states in a nucleus A and the momentum distributions in these states are given in Sec. IV. The comparison between the momentum distributions of complex nuclei and the deuteron momentum distributions is illustrated in Sec. V. In this section the result of calculation of the probability of $2N$ correlations in nuclei is also presented. Finally, the Summary and Conclusions are given in Sec. VI.

II. SPIN-ISOSPIN DEPENDENT DENSITY MATRICES, MOMENTUM DISTRIBUTIONS, AND SHORT-RANGE CORRELATIONS

A. Nuclear ground-state wave function and spin-isospin dependent density matrices

In this paper we consider the nuclear wave function of a nucleus with Z protons and N neutrons ($Z + N = A$), resulting

from the nonrelativistic Schrödinger equation containing two- and three-body interactions, viz.,

$$\left[-\frac{\hbar^2}{2m_N} \sum_{i=1} \hat{\nabla}_i^2 + \sum_{i<j} \hat{v}_2(i, j) + \sum_{i<j<k} \hat{v}_3(i, j, k) \right] \times \psi_f^A(\{\mathbf{x}_i\}_A) = E_f \psi_f^A(\{\mathbf{x}_i\}_A). \quad (1)$$

In Eq. (1) m_N is the nucleon mass, and f and $\{\mathbf{x}_i\}_A$ stand, respectively, for the set of quantum numbers of the state f , and the set of A generalized coordinates $\mathbf{x}_i \equiv \{\mathbf{r}_i, \mathbf{s}_i, \mathbf{t}_i\}$, with \mathbf{s}_i and \mathbf{t}_i denoting the nucleon spin and isospin and \mathbf{r}_i denoting the position coordinates measured from the c.m. of the nucleus ($\sum_{i=1}^A \mathbf{r}_i = 0$). Once $\psi_f^A(\{\mathbf{x}_i\}_A)$ is known, various density matrices pertaining to the nuclear ground state $\psi_{f=0}^A \equiv \psi_{JM_J}^A$ can be calculated. For ease of presentation we consider in what follows complex nuclei with zero total momentum $J = 0$ in the ground state and use the notation $\psi_{00}^A \equiv \psi_0^A$. In this paper we investigate the number of pairs in various spin-isospin states and the spin-isospin dependent two-body and one-body densities and momentum distributions. This requires the knowledge of two-body and one-body spin-isospin dependent density matrices, which can be obtained by introducing the spin-isospin projector operators $\hat{P}_{ij}^{T=1} = (3 + \boldsymbol{\tau}_i \cdot \boldsymbol{\tau}_j)/4$ and $\hat{P}_{ij}^{T=0} = (1 - \boldsymbol{\tau}_i \cdot \boldsymbol{\tau}_j)/4$, (with the same form for the spin operators). A list of the density matrices that we need in our calculations is given below:

1. *The nondiagonal spin-isospin dependent two-body density matrix, viz.,*

$$\begin{aligned} \rho_{(ST)}^{N_1 N_2}(\mathbf{r}_1, \mathbf{r}_2; \mathbf{r}'_1, \mathbf{r}'_2) &= \int \psi_0^{A*}(\tilde{\mathbf{x}}_1, \tilde{\mathbf{x}}_2, \dots, \tilde{\mathbf{x}}_A) \sum_{i<j} \hat{\rho}_{ij}^{(ST)}(\mathbf{r}_1, \mathbf{r}_2; \mathbf{r}'_1, \mathbf{r}'_2) \psi_0^A \\ &\times (\tilde{\mathbf{x}}'_1, \tilde{\mathbf{x}}'_2, \dots, \tilde{\mathbf{x}}'_A) \prod_{i=1}^A d\tilde{\mathbf{x}}_i d\tilde{\mathbf{x}}'_i, \end{aligned} \quad (2)$$

where the nondiagonal two-body spin-isospin dependent density matrix operator is

$$\begin{aligned} \hat{\rho}_{ij}^{(ST)}(\mathbf{r}_1, \mathbf{r}_2; \mathbf{r}'_1, \mathbf{r}'_2) &= \hat{P}_{ij}^S \hat{P}_{ij}^T \delta(\tilde{\mathbf{r}}_i - \mathbf{r}_1) \delta(\tilde{\mathbf{r}}_j - \mathbf{r}_2) \delta(\mathbf{r}'_1 - \tilde{\mathbf{r}}'_1) \delta(\mathbf{r}'_2 - \tilde{\mathbf{r}}'_2) \\ &\times \prod_{k \neq \{i, j\}}^A \delta(\tilde{\mathbf{r}}_k - \tilde{\mathbf{r}}'_k) \prod_{n=1}^A \delta_{s_{3n} s'_{3n}} \delta_{t_{3n} t'_{3n}}; \end{aligned} \quad (3)$$

2. *the half-diagonal two-body spin-isospin dependent density matrix, viz.,*

$$\begin{aligned} \rho_{(ST)}^{N_1 N_2}(\mathbf{r}_1, \mathbf{r}_2; \mathbf{r}'_1) &= \int \psi_0^{A*}(\tilde{\mathbf{x}}_1, \tilde{\mathbf{x}}_2, \dots, \tilde{\mathbf{x}}_A) \sum_{i<j} \hat{\rho}_{ij}^{(ST)}(\mathbf{r}_1, \mathbf{r}_2; \mathbf{r}'_1) \psi_0^A \\ &\times (\tilde{\mathbf{x}}'_1, \tilde{\mathbf{x}}'_2, \dots, \tilde{\mathbf{x}}'_A) \prod_{i=1}^A d\tilde{\mathbf{x}}_i d\tilde{\mathbf{x}}'_i, \end{aligned} \quad (4)$$

where

$$\begin{aligned} \hat{\rho}_{ij}^{(ST)}(\mathbf{r}_1, \mathbf{r}_2; \mathbf{r}'_1) &= \hat{P}_{ij}^S \hat{P}_{ij}^T \delta(\tilde{\mathbf{r}}_i - \mathbf{r}_1) \delta(\tilde{\mathbf{r}}_j - \mathbf{r}_2) \delta(\tilde{\mathbf{r}}'_i - \tilde{\mathbf{r}}'_1) \\ &\times \prod_{k \neq i}^A \delta(\tilde{\mathbf{r}}_k - \tilde{\mathbf{r}}'_k) \prod_{n=1}^A \delta_{s_{3n} s'_{3n}} \delta_{t_{3n} t'_{3n}}; \end{aligned} \quad (5)$$

3. *the diagonal two-body spin-isospin dependent density matrix, viz.,*

$$\begin{aligned} \rho_{(ST)}^{N_1 N_2}(\mathbf{r}_1, \mathbf{r}_2) &= \int \psi_0^{A*}(\tilde{\mathbf{x}}_1, \tilde{\mathbf{x}}_2, \dots, \tilde{\mathbf{x}}_A) \sum_{i<j} \hat{\rho}_{ij}^{(ST)}(\mathbf{r}_1, \mathbf{r}_2) \psi_0^A \\ &\times (\tilde{\mathbf{x}}'_1, \tilde{\mathbf{x}}'_2, \dots, \tilde{\mathbf{x}}'_A) \prod_{k=1}^A d\tilde{\mathbf{x}}_k d\tilde{\mathbf{x}}'_k, \end{aligned} \quad (6)$$

where

$$\begin{aligned} \hat{\rho}_{ij}^{(ST)}(\mathbf{r}_1, \mathbf{r}_2) &= \hat{P}_{ij}^S \hat{P}_{ij}^T \delta(\tilde{\mathbf{r}}_i - \mathbf{r}_1) \delta(\tilde{\mathbf{r}}_j - \mathbf{r}_2) \\ &\times \prod_{k=1}^A \delta(\tilde{\mathbf{r}}_k - \tilde{\mathbf{r}}'_k) \delta_{s_{3k} s'_{3k}} \delta_{t_{3k} t'_{3k}}. \end{aligned} \quad (7)$$

The following relations between the various density matrices and their normalization should be stressed:

$$\begin{aligned} \int \rho_{(ST)}^{N_1 N_2}(\mathbf{r}_1, \mathbf{r}_2; \mathbf{r}'_1, \mathbf{r}'_2) \delta(\mathbf{r}_1 - \mathbf{r}'_1) \delta(\mathbf{r}_2 - \mathbf{r}'_2) d\mathbf{r}'_1 d\mathbf{r}'_2 \\ = \rho_{(ST)}^{N_1 N_2}(\mathbf{r}_1, \mathbf{r}_2,) \end{aligned} \quad (8)$$

$$\int \rho_{(ST)}^{N_1 N_2}(\mathbf{r}_1, \mathbf{r}_2) d\mathbf{r}_1 d\mathbf{r}_2 = N_{(ST)}^A, \quad (9)$$

where $N_{(ST)}$ is the number of nucleon pairs in state (ST) , so that

$$\sum_{(ST)} N_{(ST)}^A = \frac{A(A-1)}{2} \equiv N_A. \quad (10)$$

As for the spin-isospin independent density matrices, they are normalized in the usual way, namely $\int \rho_A(\mathbf{r}_1, \mathbf{r}_2) d\mathbf{r}_1 d\mathbf{r}_2 = A(A-1)/2$, $\int \rho_A(\mathbf{r}_1, \mathbf{r}_2; \mathbf{r}'_1) d\mathbf{r}_2 = [(A-1)/2] \rho_A(\mathbf{r}_1, \mathbf{r}'_1)$, and $\int \rho_A(\mathbf{r}_1) d\mathbf{r}_1 = A$. Note that because the two-body state has to be antisymmetric, the possible ST states are $(ST) = (10), (01)$, $L = \text{even}$ and $(ST) = (11), (00)$, $L = \text{odd}$, where L is the relative orbital momentum of the pair.

B. The spin-isospin independent and spin-isospin dependent two- and one-nucleon momentum distributions

Having defined the spin-isospin dependent density matrices, we can introduce the two-body spin-isospin dependent momentum distribution of a pair of nucleons in state (ST) , namely

$$\begin{aligned} n_{(ST)}^{N_1 N_2}(\mathbf{k}_1, \mathbf{k}_2) &= \frac{1}{(2\pi)^6} \int d\mathbf{r}_1 d\mathbf{r}_2 d\mathbf{r}'_1 d\mathbf{r}'_2 e^{i\mathbf{k}_1 \cdot (\mathbf{r}_1 - \mathbf{r}'_1)} \\ &\times e^{i\mathbf{k}_2 \cdot (\mathbf{r}_2 - \mathbf{r}'_2)} \rho_{(ST)}^{N_1 N_2}(\mathbf{r}_1, \mathbf{r}_2; \mathbf{r}'_1, \mathbf{r}'_2). \end{aligned} \quad (11)$$

By summing Eq. (11) over T and S , the spin-isospin averaged two-nucleon momentum distribution is obtained¹

$$\begin{aligned} n_A(\mathbf{k}_1, \mathbf{k}_2) &= \sum_{(ST)} n_{(ST)}^{N_1 N_2}(\mathbf{k}_1, \mathbf{k}_2) \\ &= \frac{1}{(2\pi)^6} \int d\mathbf{r}_1 d\mathbf{r}'_1 d\mathbf{r}_2 d\mathbf{r}'_2 e^{i\mathbf{k}_1 \cdot (\mathbf{r}_1 - \mathbf{r}'_1)} \\ &\quad \times e^{i\mathbf{k}_2 \cdot (\mathbf{r}_2 - \mathbf{r}'_2)} \rho_A(\mathbf{r}_1, \mathbf{r}_2; \mathbf{r}'_1, \mathbf{r}'_2), \end{aligned} \quad (12)$$

where

$$\rho_A(\mathbf{r}_1, \mathbf{r}_2; \mathbf{r}'_1, \mathbf{r}'_2) = \sum_{(ST)} \rho_{(ST)}^{N_1 N_2}(\mathbf{r}_1, \mathbf{r}_2; \mathbf{r}'_1, \mathbf{r}'_2). \quad (13)$$

The two-body momentum distributions obey the following normalization:

$$\int n_{(ST)}^{N_1 N_2}(\mathbf{k}_1, \mathbf{k}_2) d\mathbf{k}_1 d\mathbf{k}_2 = \int \rho_{(ST)}^{N_1 N_2}(\mathbf{r}_1, \mathbf{r}_2) d\mathbf{r}_1 d\mathbf{r}_2 = N_{(ST)}^A \quad (14)$$

and

$$\int n_A(\mathbf{k}_1, \mathbf{k}_2) d\mathbf{k}_1 d\mathbf{k}_2 = \int \rho_A(\mathbf{r}_1, \mathbf{r}_2) d\mathbf{r}_1 d\mathbf{r}_2 = \frac{A(A-1)}{2}. \quad (15)$$

In this paper we are interested in the various spin-isospin components $n_{(ST)}^{N_1}(\mathbf{k}_1)$ of the one-body momentum distribution of nucleon N_1 ,

$$n_A^{N_1}(\mathbf{k}_1) = \frac{1}{(2\pi)^3} \frac{1}{A} \int d\mathbf{r}_1 d\mathbf{r}'_1 e^{i\mathbf{k}_1 \cdot (\mathbf{r}_1 - \mathbf{r}'_1)} \rho_A(\mathbf{r}_1, \mathbf{r}'_1), \quad (16)$$

with normalization

$$\int n_A^{N_1}(\mathbf{k}_1) d\mathbf{k}_1 = \int \rho_A^{N_1}(\mathbf{r}_1) d\mathbf{r}_1 = 1, \quad (17)$$

where $\rho_A^{N_1} = \rho_A/A$. More specifically, we have to find the spin-isospin dependent momentum distribution of a nucleon N_1 that belongs to all possible $N_1 N_2$ pairs with given value of S and T . To this end, we need the two-nucleon momentum distribution of all pairs which contains nucleon N_1 . Because the isotopic spin, unlike the spin, which is mixed by the tensor force, is a conserved quantity, we first consider the two-body momentum distribution corresponding to a fixed value of T , i.e., the spin-isospin two-body momentum distribution, Eq. (11), summed over the spin $S = 0, 1$; this quantity is denoted by $n_T^{N_1 N_2}(\mathbf{k}_1, \mathbf{k}_1)$, and, according to Pauli principle, we have

$$n_{T=0}^{N_1 N_2}(\mathbf{k}_1, \mathbf{k}_2) = [n_{(00)}^{N_1 N_2}(\mathbf{k}_1, \mathbf{k}_2) + n_{(10)}^{N_1 N_2}(\mathbf{k}_1, \mathbf{k}_2)] \quad (18)$$

and

$$n_{T=1}^{N_1 N_2}(\mathbf{k}_1, \mathbf{k}_2) = [n_{(01)}^{N_1 N_2}(\mathbf{k}_1, \mathbf{k}_2) + n_{(11)}^{N_1 N_2}(\mathbf{k}_1, \mathbf{k}_2)], \quad (19)$$

where each of the four quantities $n_{(ST)}^{N_1 N_2}(\mathbf{k}_1, \mathbf{k}_2)$ is defined by Eq. (11).

¹In case of nonisoscalar nuclei, interference between different spin-isospin states may occur. Such a contribution in case of the three nucleon systems is negligible and is omitted in the presentation.

By integrating the two-body momentum distribution in isospin state T , we find the one-body momentum distribution of a nucleon N_1 belonging to a pair with isospin T ,

$$\begin{aligned} n_T^{(N_1 N_2)}(\mathbf{k}_1) &= \frac{1}{N_T^A} \int n_T^{N_1 N_2}(\mathbf{k}_1, \mathbf{k}_2) d\mathbf{k}_2 \\ &= \frac{1}{N_T^A} \frac{1}{(2\pi)^3} \int e^{i\mathbf{k}_1 \cdot (\mathbf{r}_1 - \mathbf{r}'_1)} \\ &\quad \times \left[\int \rho_T^{N_1 N_2}(\mathbf{r}_1, \mathbf{r}_2; \mathbf{r}') d\mathbf{r}_2 \right] d\mathbf{r}_1 d\mathbf{r}'_1, \end{aligned} \quad (20)$$

with normalization

$$\int n_T^{(N_1 N_2)}(\mathbf{k}_1) d\mathbf{k}_1 = \frac{1}{N_T^A} \int n_T^{N_1 N_2}(\mathbf{k}_1, \mathbf{k}_2) d\mathbf{k}_1 d\mathbf{k}_2 = 1, \quad (21)$$

where N_T^A is the number of pairs $N_1 N_2$ with isospin T . In Eq. (20) $\rho_T^{N_1 N_2}(\mathbf{r}_1, \mathbf{r}'_1; \mathbf{r}_2)$ is the half-diagonal two-body density matrix, Eq. (4), summed over the spin; it is the central quantity necessary to calculate one-body momentum distributions. The analogs of Eqs. (18) and (19) for the T -dependent one-body momentum distribution readily follow, namely

$$n_{T=0}^{(N_1 N_2)}(\mathbf{k}_1) = [n_{(00)}^{N_1 N_2}(\mathbf{k}_1) + n_{(10)}^{N_1 N_2}(\mathbf{k}_1)], \quad (22)$$

$$n_{T=1}^{(N_1 N_2)}(\mathbf{k}_1) = [n_{(01)}^{N_1 N_2}(\mathbf{k}_1) + n_{(11)}^{N_1 N_2}(\mathbf{k}_1)]. \quad (23)$$

To obtain an explicit equation for the momentum distribution we have to know the weights of a given isospin state in nucleus A . Let us consider the proton distribution, which gets contributions from pn and pp pairs; the former can be in $T = 0$ and $T = 1$ states, whereas the latter can only be in $T = 1$ state. We have therefore to find the weight of $T = 0$ and $T = 1$ pn pairs in nucleus A , because the weight of pp pairs in $T = 1$ state is one. The total number of pn pair in $T = 0$ state in nucleus A with isospin T_A is (see Ref. [40])

$$N_{T=0}^A = N_{00}^A + N_{10}^A = \frac{1}{8} [A(A+2) - 4T_A(T_A+1)]. \quad (24)$$

Dividing Eq. (24) by the total number of pn pairs, NZ , we find the weight $w_{T=0}^{pn}$ of a pn pair in nucleus A , namely

$$w_{T=0}^{pn} = \frac{1}{8ZN} [A(A+2) - 4T_A(T_A+1)], \quad (25)$$

with the weight of a pn pair in $T = 1$ given by $w_{T=1}^{pn} = 1 - w_{T=0}^{pn}$. Thus, we obtain the momentum distribution of nucleon N_1 in terms of the explicit $T = 0, 1$ contributions

$$\begin{aligned} n_A^{N_1}(\mathbf{k}_1) &= \frac{1}{A-1} \{ Z [w_{T=0}^{pn} n_{T=0}^{(pn)}(\mathbf{k}_1) + w_{T=1}^{pn} n_{T=1}^{(pn)}(\mathbf{k}_1)] \\ &\quad + (Z-1) n_{T=1}^{(pp)}(\mathbf{k}_1) \}, \end{aligned} \quad (26)$$

which is correctly normalized to one because $w_{T=0}^{pn} + w_{T=1}^{pn} = 1$ and all $n_T^{(N_1 N_2)}(\mathbf{k}_1)$ are normalized to one

$$\int n_{T=0}^{pn}(\mathbf{k}_1) d\mathbf{k}_1 = \int n_{T=1}^{pn}(\mathbf{k}_1) d\mathbf{k}_1 = \int n_{T=1}^{pp}(\mathbf{k}_1) d\mathbf{k}_1 = 1. \quad (27)$$

Note that using Eq. (25) in Eq. (26) an even simpler equation is obtained for isoscalar nuclei, namely

$$n_A^{N_1}(\mathbf{k}_1) = \frac{1}{A-1} \left[\frac{A+2}{4} n_{T=0}^{pn}(\mathbf{k}_1) + 3 \frac{A-2}{4} n_{T=1}^{pn}(\mathbf{k}_1) \right]. \quad (28)$$

Using Eqs. (22) and (23) we can write

$$n_A^{N_1}(\mathbf{k}_1) = n_A^{(10)}(\mathbf{k}_1) + n_A^{(00)}(\mathbf{k}_1) + n_A^{(01)}(\mathbf{k}_1) + n_A^{(11)}(\mathbf{k}_1), \quad (29)$$

where all A -dependent coefficients are incorporated in the proper $n_A^{(ST)}$.

The calculation of the quantities $n_A^{(ST)}(\mathbf{k}_1)$ are presented in Sec. IV.

III. NN INTERACTIONS, MANY-BODY APPROACHES, NUCLEON MOMENTUM DISTRIBUTIONS, AND SRCs

We now address the question concerning the content of SRCs in the nuclear wave function, in particular the question concerning the definition of the probability of two-nucleon SRC, for, here, a certain degree of ambiguity may easily arise. The ground-state wave function $\psi_{JM_J}^A$ is the solution of the many-body Schrödinger equation and it describes both mean-field and correlated motions. The latter includes both long- and short-range correlations; long-range correlations manifest themselves mostly in open-shell nuclei, making partially occupied states which are empty in a simple independent particle model, with small effects on high momentum components; SRCs, however, generate high virtual particle-hole excitations even in closed-shell nuclei and strongly affect the high momentum content of the wave function. Therefore, assuming that the momentum distributions could be extracted from some experimental data, we have to figure out a clear-cut way to disentangle the momentum content generated by the mean-field from the one arising from SRCs. To this end let us use the following procedure [41]. If we denote by $\{|\psi_f^{A-1}\rangle\}$ the complete set of plane waves and eigenfunctions of the $(A-1)$ Hamiltonian of the $(A-1)$ nucleus, containing the same interaction as the Hamiltonian which generated the ground-state wave function ψ_0^A , and use the completeness relation

$$\sum_{f=0}^{\infty} |\psi_f^{A-1}\rangle \langle \psi_f^{A-1}| = 1 \quad (30)$$

in Eq. (16), it is easy to see that the one-nucleon momentum distribution becomes [41]

$$n_A^{N_1}(\mathbf{k}_1) = n_{\text{gr}}^{N_1}(\mathbf{k}_1) + n_{\text{ex}}^{N_1}(\mathbf{k}_1), \quad (31)$$

where

$$n_{\text{gr}}^{N_1}(\mathbf{k}_1) = \frac{1}{(2\pi)^3} \sum_{f=0, \sigma_1} \left| \int e^{i\mathbf{k}_1 \cdot \mathbf{r}_1} d\mathbf{r}_1 \int \chi_{\frac{1}{2}\sigma_1}^\dagger \psi_f^{(A-1)*} \times (\mathbf{r}_2, \dots, \mathbf{r}_A) \psi_0^A(\mathbf{r}_1, \mathbf{r}_2, \dots, \mathbf{r}_A) \prod_{i=2}^A d\mathbf{r}_i \right|^2 \quad (32)$$

and

$$n_{\text{ex}}^{N_1}(\mathbf{k}_1) = \frac{1}{(2\pi)^3} \sum_{f \neq 0, \sigma_1} \left| \int e^{i\mathbf{k}_1 \cdot \mathbf{r}_1} d\mathbf{r}_1 \int \chi_{\frac{1}{2}\sigma_1}^\dagger \psi_{f \neq 0}^{(A-1)*} \times (\mathbf{r}_2, \dots, \mathbf{r}_A) \psi_0^A(\mathbf{r}_1, \mathbf{r}_2, \dots, \mathbf{r}_A) \prod_{i=2}^A d\mathbf{r}_i \right|^2. \quad (33)$$

In the last equation the sum over “ f ” stands also for an integral over the continuum energy states, which are present in Eq. (30). We see that the momentum distribution can be expressed through the overlap integrals between the ground-state wave function ψ_0^A of nucleus A and the wave function $\psi_f^{(A-1)}$ of the state f of nucleus $(A-1)$. The squared modulus of the overlap integral represents the weight of the ground and excited states of $(A-1)$ in the ground state of A , so that the quantities

$$\mathcal{P}_{\text{gr}}^{N_1} = \int n_{\text{gr}}^{N_1}(\mathbf{k}_1) d\mathbf{k}_1 \quad (34)$$

and

$$\mathcal{P}_{\text{ex}}^{N_1} = \int n_{\text{ex}}^{N_1}(\mathbf{k}_1) d\mathbf{k}_1, \quad (35)$$

with

$$\mathcal{P}_{\text{gr}}^{N_1} + \mathcal{P}_{\text{ex}}^{N_1} = 1, \quad (36)$$

can be associated to the lack of ground-state correlations ($\mathcal{P}_{\text{gr}}^{N_1}$) and to the presence of them ($\mathcal{P}_{\text{ex}}^{N_1}$). The separation of the momentum distributions in $n_{\text{gr}}^{N_1}$ and $n_{\text{ex}}^{N_1}$ is particularly useful in the case of $A=3, 4$ systems, i.e., when the excited states of $(A-1)$ are in the continuum. In the case of a complex nucleus, where many discrete hole excited states are present, it is more convenient to use another representation where the particle-hole structure of the realistic solutions of Eq. (1) is explicitly exhibited, namely

$$\psi_0^A(\mathbf{r}_1, \mathbf{r}_2, \dots, \mathbf{r}_A) = c_0 \Phi_{0p0h}^A(\mathbf{r}_1, \mathbf{r}_2, \dots, \mathbf{r}_A) + c_2 \Phi_{2p2h}^A(\mathbf{r}_1, \mathbf{r}_2, \dots, \mathbf{r}_A) + \dots \quad (37)$$

In Eq. (37), Φ_{0p0h}^A is a Slater determinant describing the mean field motion of A nucleons occupying all states below the Fermi level, Φ_{2p2h}^A describes 2p-2h excitations owing to SRC, and the dots include higher order p-h excitations. The modulus squared of the various expansion coefficients c_i is nothing but the probability to have np - nh excitations in the ground-state wave function. In particular $|c_2|^2 \equiv a_2$ will determine the amount of ground-state SRCs. Within such a representation, one can write [42]

$$n_A^{N_1}(\mathbf{k}_1) = n_0^{N_1}(\mathbf{k}_1) + n_1^{N_1}(\mathbf{k}_1), \quad (38)$$

where

$$n_0^{N_1}(\mathbf{k}_1) = \frac{1}{(2\pi)^3} \sum_{f \leq F, \sigma_1} \left| \int e^{i\mathbf{k}_1 \cdot \mathbf{r}_1} d\mathbf{r}_1 \int \chi_{\frac{1}{2}\sigma_1}^\dagger \psi_f^{(A-1)*} \times (\mathbf{r}_2, \dots, \mathbf{r}_A) \psi_0^A(\mathbf{r}_1, \mathbf{r}_2, \dots, \mathbf{r}_A) \prod_{i=2}^A d\mathbf{r}_i \right|^2 \quad (39)$$

and

$$n_1^{N_1}(\mathbf{k}_1) = \frac{1}{(2\pi)^3} \sum_{f>F, \sigma_1} \left| \int e^{i\mathbf{k}_1 \cdot \mathbf{r}_1} d\mathbf{r}_1 \int \chi_{\frac{1}{2}\sigma_1}^\dagger \psi_f^{(A-1)*} \times (\mathbf{r}_2, \dots, \mathbf{r}_A) \psi_0^A(\mathbf{r}_1, \mathbf{r}_2, \dots, \mathbf{r}_A) \prod_{i=2}^A d\mathbf{r}_i \right|^2, \quad (40)$$

where the summation over f in Eq. (39) includes all the discrete shell-model levels below the Fermi level (F) in $(A-1)$ (“hole states” of A), and in Eq. (40) it includes all the discrete and continuum states above the Fermi sea created by SRCs. In a fully uncorrelated mean-field approach, we have

$$n_A^{N_1}(\mathbf{k}_1) = n_0^{N_1}(\mathbf{k}_1) = \sum_{\alpha \leq F} |\phi_\alpha(\mathbf{k}_1)|^2; \quad n_1^{N_1}(k_1) = 0, \quad (41)$$

and the the analogs of Eqs. (34) and (35) are

$$\mathcal{P}_0^{N_1} = \int n_0^{N_1}(\mathbf{k}_1) d\mathbf{k}_1, \quad (42)$$

$$\mathcal{P}_1^{N_1} = \int n_1^{N_1}(\mathbf{k}_1) d\mathbf{k}_1, \quad (43)$$

with

$$\mathcal{P}_0^{N_1} + \mathcal{P}_1^{N_1} = 1. \quad (44)$$

$$S_A^{N_1}(\mathbf{k}_1, E) = \langle \psi_0^A | a_{\mathbf{k}_1, \sigma_1}^\dagger \delta(E - \hat{H} + E_A) a_{\mathbf{k}_1, \sigma_1} | \psi_0^A \rangle \quad (46)$$

$$= \sum_{f, \sigma_1} \left| \int e^{i\mathbf{k}_1 \cdot \mathbf{r}_1} d\mathbf{r}_1 \int \chi_{\frac{1}{2}\sigma_1}^\dagger \psi_f^{(A-1)*}(\mathbf{r}_2, \dots, \mathbf{r}_A) \psi_0^A(\mathbf{r}_1, \mathbf{r}_2, \dots, \mathbf{r}_A) \prod_{i=2}^A d\mathbf{r}_i \right|^2 \delta[E - E_{A-1}^f - E_A] \quad (47)$$

$$= S_0^{N_1}(\mathbf{k}_1, E_0) + S_1^{N_1}(\mathbf{k}_1, E), \quad (48)$$

where Eq. (48) has been obtained from Eq. (47) using the completeness relation [Eq. (30)], $a_{\mathbf{k}_1}^\dagger$ ($a_{\mathbf{k}_1}$) is a creation (annihilation) operator, $E_A = M_A - M_{A-1} - m_N$, $E = E_A + E_{A-1}^f$ is the nucleon removal energy, and

$$S_0^{N_1}(\mathbf{k}_1, E) = \sum_{f \leq F} \left| \int e^{i\mathbf{k}_1 \cdot \mathbf{r}_1} d\mathbf{r}_1 \int \chi_{\frac{1}{2}\sigma_1}^\dagger \psi_f^{(A-1)*}(\mathbf{r}_2, \dots, \mathbf{r}_A) \times \psi_0^A(\mathbf{r}_1, \mathbf{r}_2, \dots, \mathbf{r}_A) \prod_{i=2}^A d\mathbf{r}_i \right|^2 \times \delta(E - E_{A-1}^f - E_A), \quad (49)$$

$$S_1^{N_1}(\mathbf{k}_1, E) = \sum_{f>0} \left| \int e^{i\mathbf{k}_1 \cdot \mathbf{r}_1} d\mathbf{r}_1 \int \chi_{\frac{1}{2}\sigma_1}^\dagger \psi_f^{(A-1)*}(\mathbf{r}_2, \dots, \mathbf{r}_A) \times \psi_0^A(\mathbf{r}_1, \mathbf{r}_2, \dots, \mathbf{r}_A) \prod_{i=2}^A d\mathbf{r}_i \right|^2 \times \delta(E - E_{A-1}^f - E_A). \quad (50)$$

The spectral function represents the probability that, after particle “1” is adiabatically removed from the bound state

The quantities $\mathcal{P}_0^{N_1}$ and $\mathcal{P}_1^{N_1}$ yield, respectively, the probability to find a mean-field and a correlated nucleon in the range $0 \leq k_1 \leq \infty$. Therefore, they can be assumed as the mean-field and SRC total probabilities. It is clear that both low- and high-momentum components contribute to mean-field and correlated momentum distributions, but we shall see, as expected, that $n_0^{N_1}$ ($n_1^{N_1}$) gets contribution mainly from low- (high-) momentum components. Assuming that $n_0^{N_1}$ and $n_1^{N_1}$ could experimentally be obtained, it might well be that only a limited range of momenta is available experimentally, in which case it is useful to define the partial probabilities

$$\mathcal{P}_{0(1)}^{N_1}(k_1^\pm) = 4\pi \int_{k_1^-}^{k_1^+} n_{0(1)}^{N_1}(\mathbf{k}_1) k_1^2 d k_1, \quad (45)$$

i.e., the probability to observe a mean-field (correlated) nucleon with momentum in the range $k_1^- \leq k_1 \leq k_1^+$. Although we do not discuss in this paper how the momentum distribution could, in principle, be extracted from the experimental data, we would like nevertheless to briefly comment on this point. It is clear from the very definition of the momentum distribution that to obtain information on it one has to figure out an experiment in which a nucleon is struck from a nucleus A and the nucleus $(A-1)$ is left in a well-defined energy state. To fully understand the point, it is useful to introduce the nucleon spectral function, i.e., the following quantity:

and placed in the continuum, the nucleus $(A-1)$ remains in the state E_{A-1}^f . The relation between the spectral function and the momentum distribution is given by the momentum sum rule

$$\int S_A^{N_1}(\mathbf{k}_1, E) dE = n_A^{N_1}(\mathbf{k}_1). \quad (51)$$

The partial and full momentum distributions can therefore be obtained, in principle, by detecting the final nuclear system $(A-1)$ in correspondence of $f \leq F$ and $f > F$. The exclusive processes $A(e, e'N)(A-1)_f$ in plane wave impulse approximation (PWIA) depends directly upon $S(\mathbf{k}_1, E)$. Thus, by performing these types of experiments in a wide range of excitation energies of the final $(A-1)$ nucleus and by performing the integration over E the momentum distributions can be obtained. FSIs make the cross section deviate from the PWIA, and, moreover, for a complex nucleus, the sum over the entire continuum spectrum of $(A-1)$ is difficult, if not impossible, to perform. In the case of few-body systems this difficulty can be overcome, because the number of possible final states is strongly reduced and, as a matter of fact, experimental information of n_{gr} and n_{ex} for ${}^3\text{He}$ and ${}^4\text{He}$ is already available [43,44].

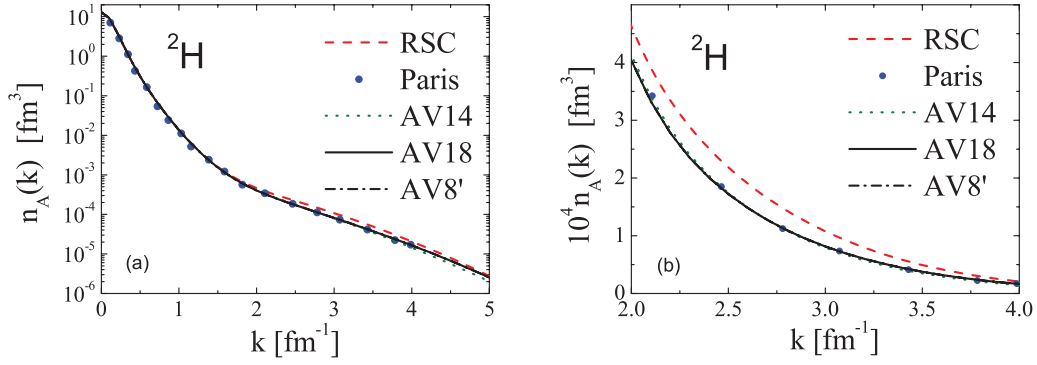


FIG. 1. (Color online) Deuteron momentum distributions in logarithmic (a) and linear (b) scales corresponding to various NN interactions: RSC [35], Paris [36], AV8' [37], AV14 [38], and AV18 [39]. Unless otherwise stated, here and in the other figures, the normalization is $4\pi \int k^2 dk n_A(k) = 1$. In this and the following figures $|\mathbf{k}_1| \equiv k$ and $n_A(k) \equiv n_A^{N_1}(k)$ [Eq. (16)].

We reiterate that the aim of this paper is the theoretical investigation of some general properties of momentum distributions, concerning in particular their SRC and spin-isospin structures. To this end for $A = 3$ and 4 “exact” wave functions obtained, either by a direct solution of the Schrödinger equation or by variational procedures, are used, whereas for complex nuclei momentum distributions obtained from various methods, ranging from the Brueckner-Bethe-Goldstone approach to the cluster expansion techniques, are adopted. In the next section the momentum distributions of several nuclei are presented and the values of the quantity $\mathcal{P}_{0(1)}^{N_1}(k_{1}^{\pm})$ [Eq. (45)] are given.

A. The momentum distributions of few-nucleon systems and complex nuclei

In this section the momentum distributions of ${}^2\text{H}$, ${}^3\text{H}$, ${}^3\text{He}$, ${}^4\text{He}$, ${}^{16}\text{O}$, and ${}^{40}\text{Ca}$, calculated within different approaches and using various two-nucleon interactions, will be presented. The full momentum distributions are shown in Figs. 1–6, whereas their separation into the mean-field and correlation contributions, according to Eqs. (32), (33), (39), and (40), are presented in Figs. 7–10. Note that from now on the notation $\mathbf{k} \equiv \mathbf{k}_1$ and $k \equiv |\mathbf{k}_1|$ is used.

1. The momentum distributions of ${}^2\text{H}$

The momentum distributions of ${}^2\text{H}$ obtained by solving exactly the Schrödinger equation is crucial for our analysis. It is presented in Fig. 1, where it can be seen that, apart from the RSC interaction [35], the Paris interaction [36] and the family of Argonne interactions AV8' [37], AV14 [38], and AV18 [39] provide essentially the same result. All these potentials exhibit a strong short-range repulsion which gives rise to a strong suppression of the deuteron wave function at internucleon separation $r = |\mathbf{r}_1 - \mathbf{r}_2| \lesssim 1.5$ fm. This, together with the effects from the tensor force, generate high-momentum components in the momentum distribution.

2. The momentum distributions of ${}^3\text{H}$ and ${}^3\text{He}$

As already stated in Sec. III, the three- and four-nucleon systems ${}^3\text{H}$, ${}^3\text{He}$, and ${}^4\text{He}$ are very important in that n_{gr} and n_{ex} have been explicitly calculated within accurate few-body techniques. Moreover, being ${}^3\text{He}$ and ${}^3\text{H}$ nonisospin nuclei, their proton and neutron distributions are different. As a matter of fact, in ${}^3\text{He}$ the proton momentum distribution is given by

$$n_3^p(k) = n_3^p(k) + n_{\text{ex}}^p(k) \quad (52)$$

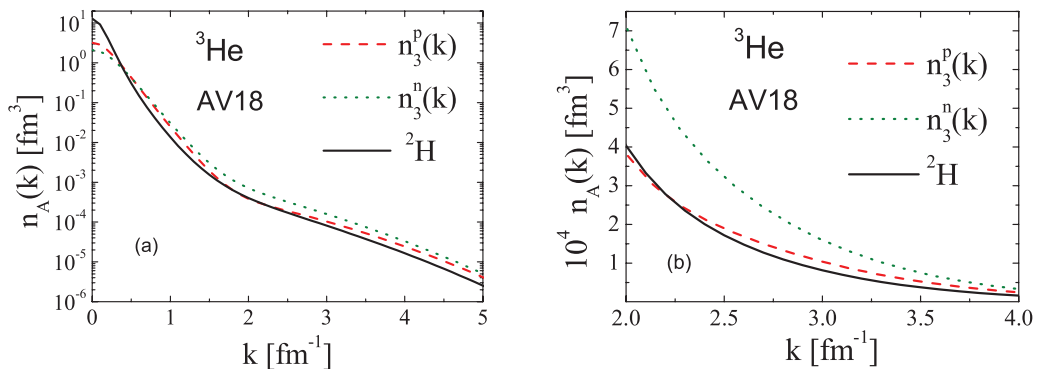


FIG. 2. (Color online) The proton and neutron momentum distributions of ${}^3\text{He}$ in logarithmic (a) and linear (b) scales. Three-nucleon wave functions from Ref. [26]. The full curve represents the deuteron momentum distribution. Both ${}^3\text{He}$ and deuteron wave functions correspond to the AV18 interaction [39].

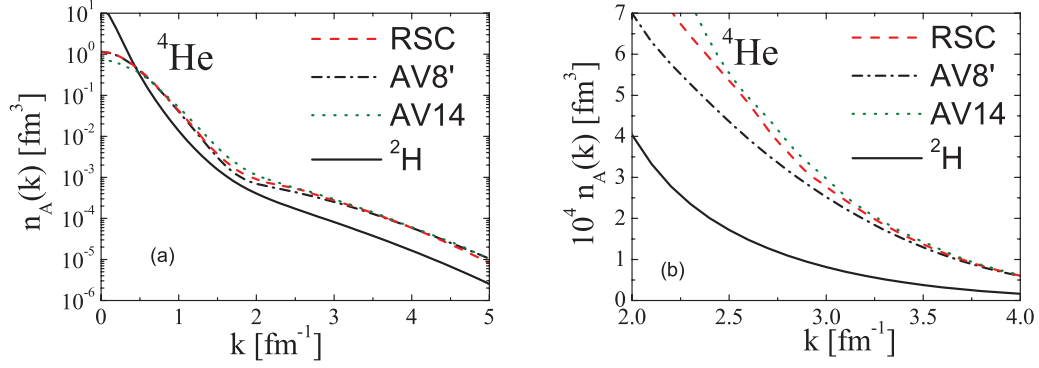


FIG. 3. (Color online) The nucleon momentum distributions of ${}^4\text{He}$ in logarithmic (a) and linear (b) scales corresponding to different four-body wave functions and NN interactions. Dashed curve, Ref. [24]; dot-dashed curve, Ref. [25]; dotted curve, Ref. [22]. The full curve represents the deuteron momentum distribution corresponding to the AV18 interaction.

and the neutron distribution, owing to the absence of a two-body bound state in the final state [cf. Eq. (33)], is given by

$$n_3^n(k) = n_{\text{ex}}^n(k). \quad (53)$$

In the above equations, $n_{\text{gr}}^p(k)$ is the Fourier transform of the overlap between the ground-state wave functions of ${}^3\text{He}$ and ${}^2\text{H}$ [cf. Eq. (32)] and $n_{\text{ex}}^p(k)$ is the Fourier transform of the overlap between the ground-state wave function of ${}^3\text{He}$ and the continuum state of pn pair [cf. Eq. (33)]. Thanks to isospin invariance, Eqs. (52) and (53) represent, respectively, the neutrons and protons momentum distributions in ${}^3\text{H}$. The proton and neutron momentum distributions in ${}^3\text{He}$ resulting from Faddeev and variational calculations in correspondence of the AV18 interaction are shown in Fig. 2. It can indeed be seen that they are different, with the former strongly differing from the deuteron momentum distributions. The origin of such a difference is discussed in detail in Sec. IV.

3. The momentum distributions of ${}^4\text{He}$

The nucleus ${}^4\text{He}$ is the lightest isoscalar nucleus, with identical proton and neutron momentum distributions. These have been calculated in Ref. [25] within the approach of Ref. [24] using the AV8' interaction. They are compared in

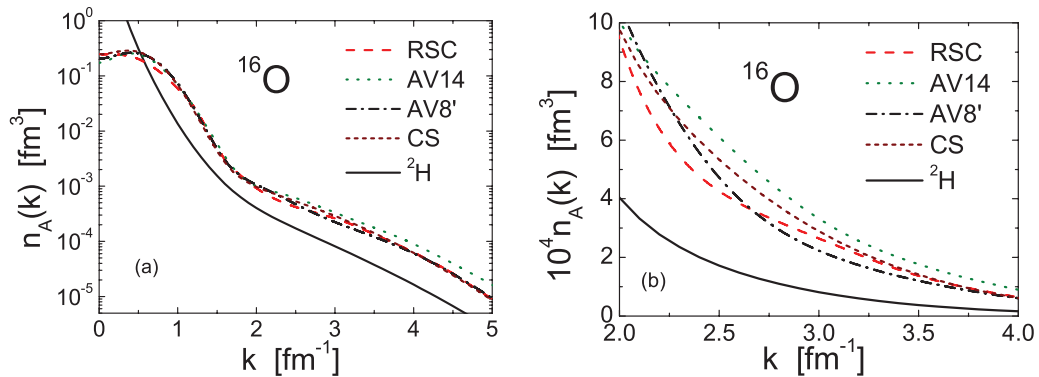


FIG. 4. (Color online) The momentum distribution of ${}^{16}\text{O}$ in logarithmic (a) and linear (b) scales, corresponding to different wave functions and NN interactions: Dashed curve, Ref. [17]; dotted curve, Ref. [22]; dot-dashed curve, Ref. [31]. The parametrization of Ref. [12] is also shown by the short-dashed curve (CS). The full curve represents the deuteron momentum distribution corresponding to the AV18 interaction.

Fig. 3 with the results of the variational Monte Carlo method performed with the AV14 interaction [22].

4. The momentum distributions of ${}^{16}\text{O}$ and ${}^{40}\text{Ca}$

The momentum distributions of complex nuclei is by far more complicated to calculate with the same accuracy attained in the case of three- and four-nucleon systems. Nonetheless, several calculations for ${}^{16}\text{O}$ have been performed within different approaches and using various NN interactions, namely with the RSC potential [35], in Refs. [17–20], with the AV8' potential [37], in Refs. [28] and [31], and with the AV14 potential [38] in Ref. [22]; the various methods that have been used are the unitary operator approach [17], the Brueckner-Bethe-Goldstone approach [18,20], the cluster expansion approach truncated at different orders [19,31], the fermion-hypernetted-chain method [28], and the variational Monte Carlo correlated approach [22]. The various results are compared in Fig. 4. As for ${}^{40}\text{Ca}$, two available results obtained with the V8' interactions are shown in Fig. 5.

5. The A -dependence of the momentum distributions

The momentum distributions of the considered nuclei obtained with the V8' interaction (the AV18 in the ${}^2\text{H}$ and

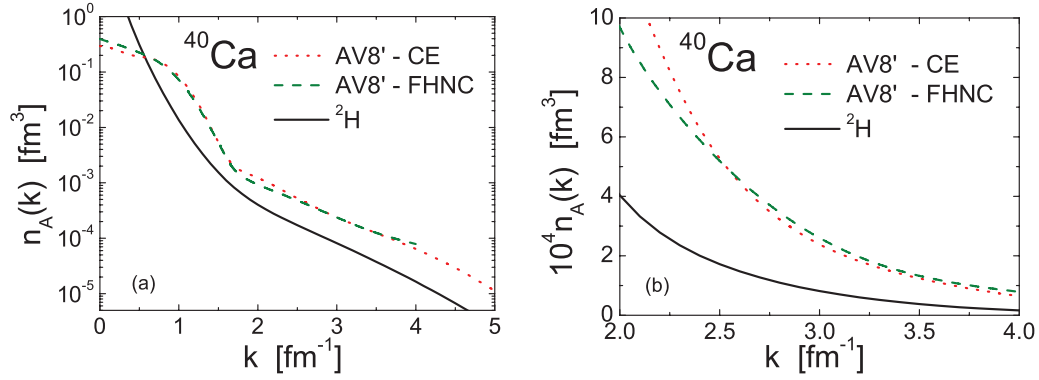


FIG. 5. (Color online) The momentum distribution of ^{40}Ca in logarithmic (a) and linear (b) scales, corresponding to the AV8' NN interaction calculated within two different many-body approaches. Dashed curve, cluster expansion (FHNC) up to FHNC/SOC order [28]; dotted curve, cluster expansion (CE) at second order [31]. The full curve represents the deuteron momentum distribution corresponding to the AV18 interaction.

^3He cases) are compared in Fig. 6. The general features that emerge from such a comparison can be summarized as follows. (i) At low values of the momentum $k = |\mathbf{k}_1|$ the shape of $n_A(k)$ is determined by the asymptotic behavior of the wave function of the least bound nucleon, and therefore it is very different for different nuclei. (ii) In the high-momentum region ($k \gtrsim 1.5\text{--}2\text{ fm}^{-1}$) a qualitative similarity between the momentum distributions of deuteron and heavier nuclei can be observed. In what follows we show that in this region $n_A(k)$ is dominated by the correlated part of the distributions, namely n_{ex} and n_1 , and that the similarity between deuteron and complex nuclei is only a qualitative one, with the high-momentum behavior of $n_A(k)$ being governed by the various spin-isospin components contributing to $n_A(k)$, and not only by the deuteronlike state ($ST) = (10)$.

6. The mean-field and SRC contributions to the momentum distributions

The separation of the momentum distribution according to Eqs. (31) and (38) is shown in Figs. 7–10. It can be seen that (i) in the region $k \lesssim 1.5\text{--}2.0\text{ fm}^{-1}$ SRCs reduce the mean-field distribution without practically changing its shape, the effect being attributable to the decrease of the occupation probability

of the shell-model states below the Fermi level; (ii) in the region $k \gtrsim 2.0\text{ fm}^{-1}$ the momentum distributions are entirely exhausted by SRCs. Having at disposal both $n_{gr}(k)$ [$n_0(k)$] and $n_{ex}(k)$ [$n_1(k)$] the probabilities given by Eqs. (34), (35), (42), and (43) can be calculated. These are listed in Table I, whereas the partial probabilities defined by Eq. (45) are listed in Table II.

B. Summary of Sec. II

From what is exhibited in the present section, some general features of the momentum distributions can be identified, which are, to a large extent, independent of the many-body approach and the two-nucleon interaction used in the calculations, namely: (i) at $k \gtrsim 2\text{ fm}^{-1}$ the momentum distributions of both few-nucleon and complex nuclei qualitatively resemble the deuteron momentum distributions; (ii) in the region of high momenta, the realistic momentum distributions of complex nuclei overwhelm the mean-field distributions by several orders of magnitude; (iii) whereas for few-nucleon systems the method of calculations is very well established, for complex nuclei different methods and potentials provide at high momenta values of the distributions which can differ up to a factor of two, and it is not yet clear to which extent

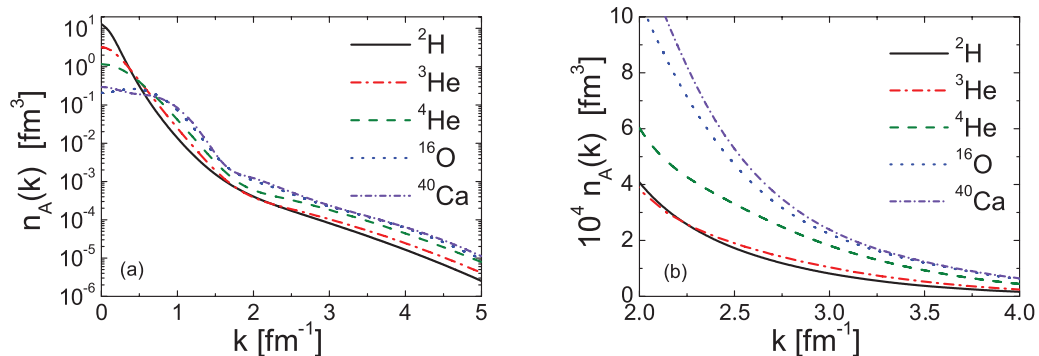


FIG. 6. (Color online) The proton momentum distribution of nuclei considered in this work in logarithmic (a) and linear (b) scales, calculated within different many-body approaches with equivalent NN interactions, namely the AV18 one, in the case of ^2H and ^3He , and the AV8' one, in the case of ^4He , ^{16}O , and ^{40}Ca .

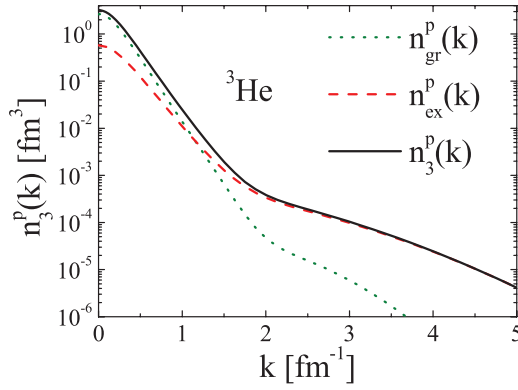


FIG. 7. (Color online) The separate contributions n_{gr} and n_{ex} to the proton momentum distributions of ${}^3\text{He}$. Wave function from Ref. [26], AV18 interaction. The values of $\mathcal{P}_{\text{gr}}^p = 4\pi \int k^2 dk n_{\text{gr}}^p(k)$ and $\mathcal{P}_{\text{ex}}^p = 4\pi \int k^2 dk n_{\text{ex}}^p(k)$ are listed in Table I, and the values of Eq. (45) in Table II.

such a difference should be ascribed to the different potentials or to the different methods. It should be mentioned that the momentum distributions extracted from $A(e, e'p)X$ and from the y -scaling analysis of inclusive $A(e, e')X$ scattering [16] agree with many-body calculations; although the errors of the extracted momentum distributions are very large at high momenta, they are much smaller than the difference between correlated and mean-field distributions, with the latter being totally inadequate to predict high-momentum components. In what follows our analysis of the momentum distributions continues using the most advanced available calculation methods and two-nucleon interactions. To understand the microscopic origin of the correlated part of $n_A(k)$, we analyze in the next section its spin-isospin structure.

IV. THE SPIN-ISOSPIN STRUCTURE OF THE NUCLEON MOMENTUM DISTRIBUTION AND SRC

The spin-isospin structure of SRCs is a fundamental quantity because it reflects the details of the NN interaction in the medium. It is therefore important to investigate how such

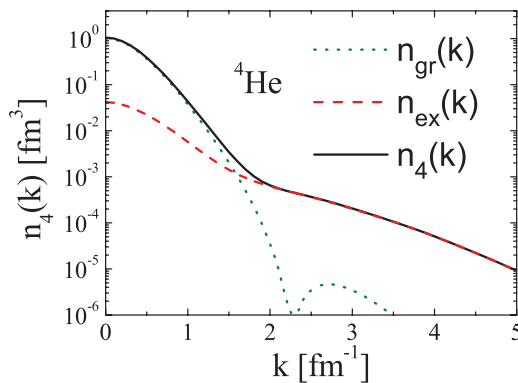


FIG. 8. (Color online) The same as in Fig. 7 but for ${}^4\text{He}$. Wave function from Ref. [25], AV8' interaction. The values of $\mathcal{P}_{\text{gr}} = 4\pi \int k^2 dk n_{\text{gr}}(k)$ and $\mathcal{P}_{\text{ex}} = 4\pi \int k^2 dk n_{\text{ex}}(k)$ are listed in Table I, and the values of Eq. (45) in Table II.

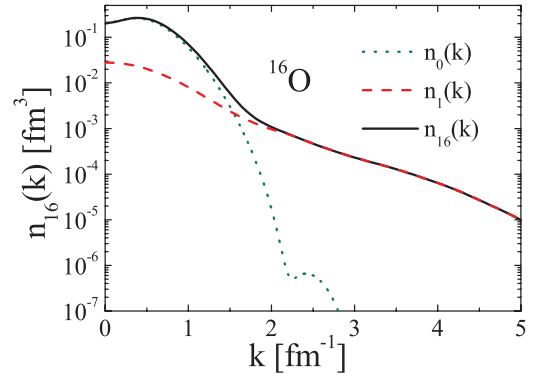


FIG. 9. (Color online) The same as in Fig. 7 but for ${}^{16}\text{O}$. Wave functions from Ref. [31], AV8' interaction. The values of $\mathcal{P}_0 = 4\pi \int k^2 dk n_0(k)$ and $\mathcal{P}_1 = 4\pi \int k^2 dk n_1(k)$ are listed in Table I, and the values of Eq. (45) in Table II.

a structure can affect various quantities which are related to SRCs, such as, e.g., the nucleon momentum distributions. In Ref. [23] a detailed analysis pertaining to few-nucleon systems has been presented of the various (ST) channel contributions to the relative momentum distribution $n_{(ST)}^{N_1 N_2}(\mathbf{k}_1, \mathbf{k}_2)$, Eq. (11), integrated over the c.m. momentum, namely,

$$\begin{aligned} n_{(ST)}^{N_1 N_2}(\mathbf{k}_{\text{rel}}) &= \int n_{(ST)}^{N_1 N_2}(\mathbf{k}_1, \mathbf{k}_2) d\mathbf{K}_{\text{c.m.}} \\ &= \int n_{(ST)}^{N_1 N_2}(\mathbf{k}_{\text{rel}}, \mathbf{K}_{\text{c.m.}}) d\mathbf{K}_{\text{c.m.}}, \end{aligned} \quad (54)$$

whereas in Ref. [11] the dependence of the two-body momentum distribution $n_{(ST)}^{N_1 N_2}(\mathbf{k}_1, \mathbf{k}_2) = n_{(ST)}^{N_1 N_2}(k_{\text{rel}}, K_{\text{c.m.}}, \theta)$, upon the values of k_{rel} , $K_{\text{c.m.}}$, and θ has been investigated in the case of $A = 3$ and 4.

In this paper we proceed further on into this direction by analyzing the contribution of various (ST) channels to the one-body momentum distribution of a nucleon N_1 belonging to a $N_1 N_2$ pair in a spin-isospin state (ST) . Our aim is to understand the quantitative relevance and the momentum dependence of these contributions, in particular as far as the deuteronlike state (10) is concerned. In this respect, it should be stressed that in Ref. [11], it has been shown that in ${}^3\text{He}$ and ${}^4\text{He}$

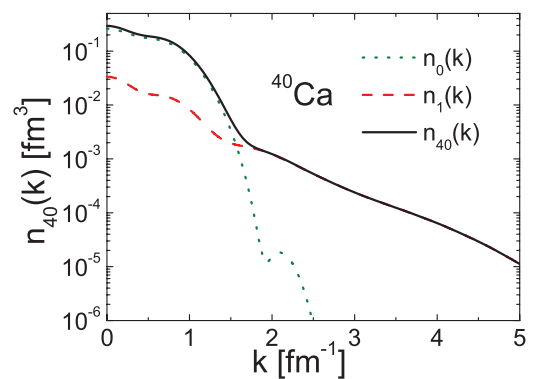


FIG. 10. (Color online) The same as in Fig. 7 but for ${}^{40}\text{Ca}$. Wave function from Ref. [31], AV8' interaction. The values of $S_0 = 4\pi \int k^2 dk n_0(k)$ and $S_1 = 4\pi \int k^2 dk n_1(k)$ are listed in Table I, and the values of Eq. (45) in Table II.

TABLE I. The proton mean-field and correlation probabilities $\mathcal{P}_{\text{gr}(0)}^p = \int d\mathbf{k}_1 n_{\text{gr}(0)}^p(\mathbf{k}_1)$ [Eqs. (34) and (42)] and $\mathcal{P}_{\text{ex}(1)}^p = \int d\mathbf{k}_1 n_{\text{ex}(1)}^p(\mathbf{k}_1)$ [Eqs. (35) and (43)].

Nucleus	Potential	\mathcal{P}_{gr}	\mathcal{P}_{ex}
^3He [26]	AV18 [39]	0.677	0.323
^4He [21,24]	RSC [35] AV8' [37]	0.85	0.15
		\mathcal{P}_0	\mathcal{P}_1
^{16}O [22]	V8' [37]	0.8	0.2
^{40}Ca [11]	V8' [37]	0.8	0.2

and for back-to-back nucleons ($K_{\text{c.m.}} = 0$, the deuteronlike momentum configuration) the quantity

$$R_{(10)}^{(pn)}(k_{\text{rel}}, K_{\text{c.m.}} = 0) = n_{(10)}^{pn}(k_{\text{rel}}, K_{\text{c.m.}} = 0)/n_D(k_{\text{rel}}), \quad (55)$$

i.e., the ratio of the relative momentum distribution of a pn pair in state (ST) = (10) to the deuteron momentum distribution, exhibits a constant behavior starting from $k_{\text{rel}} \gtrsim 1.5\text{--}2 \text{ fm}^{-1}$; this means that at short relative distances, the motion of a back-to-back (pn) pair in a nucleus behaves like in a deuteron. However, a constant behavior is not expected to be observed in the ratio of the (ST) one-nucleon momentum distribution to the deuteron distribution, because the former, being the integral of the two-body momentum distribution, besides the deuteronlike configuration, includes many other NN configurations. The separation of various (ST) contributions to the one-body momentum distribution is an involved task. The problem can be solved by considering the half-diagonal spin-isospin dependent two-body density matrix and its integral over \mathbf{r}_2 . To this end, it is useful first of all to calculate the number of nucleon pairs in a given spin-isospin state.

A. The number of NN pairs in various spin-isospin states

The two-body interaction acts differently in states with different spin, isospin, and relative orbital momentum L , whose values are fixed by the Pauli principle, namely $S + T + L = \text{odd}$. To investigate the spin-isospin dependence of the momentum distributions, it is useful to start counting the number of pairs $N_{(ST)}^{N_1 N_2}$ in various (ST) states in a nucleus with Z protons and N neutrons, with $Z + N = A$. This quantity is given by Eq. (9) and satisfies the sum rule Eq. (10). The value of $N_{(ST)}^{N_1 N_2}$ has been calculated in various papers, e.g., in Refs. [40,45] for $A \leq 16$, in Ref. [23] for $A \leq 4$ and in

Refs. [46,47]. Here our approach to this topic and the results for $A = 3, 4, 16$, and 40 and $L = \text{even}$ and odd will be presented.

To start with, let us consider a full independent-particle (IP) shell model. In the case of s -shell nuclei the number of pairs in (ST) states can readily be obtained. As a matter of fact, in $A = 3$ and 4 nuclei the relative orbital momentum of all pairs is zero, so that only two (ST) states survive, namely (10) and (01). A pn pair can be either in (10) state, with probability $3/4$, or in (01) state, with probability $1/4$, whereas a $pp(nn)$ pair can only be in (01) state, with probability 1. Multiplying these probabilities by the number of pn , pp , and nn pairs [NZ , $Z(Z-1)/2$, $N(N-1)/2$, respectively], the total number of pairs is obtained

$$N_{3(4)} = NZ \left(\frac{3}{4}(10)_{pn} + \frac{1}{4}(01)_{pn} \right) + \frac{Z(Z-1)}{2}(01)_{pp} + \frac{N(N-1)}{2}(01)_{nn}, \quad (56)$$

with the total number of pairs in a given (ST) given by

$$N_{(10)}^3 = \frac{3}{2}, \quad N_{(01)}^3 = \frac{3}{2}, \quad (57)$$

in ^3He , and

$$N_{(10)}^4 = 3, \quad N_{(01)}^4 = 3, \quad (58)$$

in ^4He (note that the state (10) refers to pn pairs only, whereas the state (01) includes pp , nn , and pn pairs and it is for this reason that no nucleon labels appear in $N_{(ST)}$). In $A > 4$ nuclei also the states (11) and (00) contribute. In Ref. [45] a general approach to calculate, within the IP model, the number of pairs in various (ST) states, based upon counting even and odd pairs in spatial configurations corresponding to a given Young tableaux, has been given, and explicit formulas can be found there. In our approach the values of $N_{(ST)}^A$, for the three- and four-nucleon systems have been obtained using the wave functions of Ref. [24–26] corresponding to the AV18 and AV8' interaction, respectively, whereas for complex nuclei the cluster expansion of Ref. [31] which includes two-, three-, and four-body cluster contributions has been used to calculate the integral of the diagonal spin-isospin dependent two-body density matrix [Eq. (6)] yielding

$$N_{(ST)}^A = \int \rho_{(ST)}^{N_1 N_2}(\mathbf{r}_1, \mathbf{r}_2) d\mathbf{r}_1 d\mathbf{r}_2 = \int n_{(ST)}^{N_1 N_2}(\mathbf{k}_1, \mathbf{k}_2) d\mathbf{k}_1 d\mathbf{k}_2 = \int n_{(ST)}^{N_1 N_2}(\mathbf{k}_{\text{rel}}, \mathbf{k}_{\text{c.m.}}) d\mathbf{k}_{\text{rel}} d\mathbf{K}_{\text{c.m.}}. \quad (59)$$

TABLE II. The values of the partial probability, Eq. (45), for ^3He , ^4He , ^{16}O , and ^{40}Ca , calculated for different values of the momentum k_1^- with $k_1^+ = \infty$.

k_1^- (fm $^{-1}$)	^2H	$^3\text{He}(n)$	$^3\text{He}(p)$		^4He		^{16}O		^{40}Ca	
	\mathcal{P}	\mathcal{P}_1	\mathcal{P}_0	\mathcal{P}_1	\mathcal{P}_0	\mathcal{P}_1	\mathcal{P}_0	\mathcal{P}_1	\mathcal{P}_0	\mathcal{P}_1
0.00	1.000	0.999	0.677	0.323	0.846 21	0.152 85	0.799 99	0.200 16	0.80	0.193 21
0.50	0.3078	0.568	0.277	0.201	0.536 43	0.140 32	0.669 72	0.196 35	0.699 97	0.183 01
1.00	0.081	0.163	0.038	0.0723	0.104 79	0.1045	0.175 88	0.147 94	0.247 06	0.137 71
1.50	0.0366	0.067	0.0049	0.036	0.0079	0.0791	0.007 92	0.094 17	0.010 22	0.101 43
2.00	0.0221	0.041	0.0015	0.024	6.9512×10^{-4}	0.061 56	5.9×10^{-5}	0.063 44	3.28×10^{-4}	0.071 24

TABLE III. The number of pairs $N_{(ST)}^A$, Eq. (9) in various spin-isospin states in the independent particle model (IPM) and taking into account SRCs within many-body theories with realistic interactions (in the approach of Ref. [46] pairs in relative $L = 0$ motion were identified as those prone to SRCs).

Nucleus		(ST)			
		(10)	(01)	(00)	(11)
^2H		1	—	—	—
^3He	IPM	1.50	1.50	—	—
	SRC (Present work)	1.488	1.360	0.013	0.139
	SRC [40]	1.50	1.350	0.01	0.14
	SRC [23]	1.489	1.361	0.011	0.139
^4He	IPM	3	3	—	—
	IPM ($0s$ states) [46]	3	3	—	—
	SRC (Present work)	2.99	2.57	0.01	0.43
	SRC [40]	3.02	2.5	0.01	0.47
	SRC [23]	2.992	2.572	0.08	0.428
^{16}O	IPM	30	30	6	54
	IPM ($0s$ states) [46]	20	18	—	—
	SRC (Present work)	29.8	27.5	6.075	56.7
	SRC [40]	30.05	28.4	6.05	55.5
^{40}Ca	IPM	165	165	45	405
	IPM ($0s$ states) [46]	90	20	—	—
	SRC (Present work)	165.18	159.39	45.10	410.34

If IP wave functions are used in Eq. (59), the IP values of $N_{(ST)}^A$ have to coincide with the values provided by the formulas of Ref. [45], as indeed it is the case. When the IP model picture is released and a full many-body approach with interacting nucleons is considered, odd values of the relative orbital momentum appear also in $A = 3$ and 4 nuclei so that (i) the states (00) and (11) are generated in ^3H , ^3He , and ^4He ; (ii) the amount of various (ST) states in complex nuclei is changed. Thanks to isospin conservation, the number of states (01) is decreased in favor of states (11) and the number of deuteronlike states (10) is also decreased in favor of the state (00). In Ref. [40] $N_{(ST)}^{N_1N_2}$ has been calculated for ^3He , ^4He , ^6Li , ^7Li , and ^{16}O using variational Green's functions Monte Carlo wave functions and various Argonne interactions; in Ref. [23] $N_{(ST)}^A$ has been obtained for nuclei ^3He , ^3H , and ^4He using wave functions resulting from the correlated Gaussian basis approach [32] and the V8' interaction, finally, in Refs. [46,47] the number of pairs has been evaluated through the periodic table using phenomenological correlated wave functions. We reiterate that in the present paper we have calculated $N_{(ST)}^A$ for $A = 3, 4, 16, 40$ using wave functions obtained within the hyperspherical harmonic variational method [26] and the AV18 interaction, for $A = 3$, the ATMS method of Refs. [24,25] and the AV8' interaction, for $A = 4$, the linked-cluster expansion of Ref. [31] and the AV8', for $A = 16$ and $A = 40$. The results of our calculations, which are presented in Table III, clearly show that (i) there is satisfactory general agreement between our results and the ones of Ref. [23,40]; (ii) as previously found in those papers, when the IP model picture is released and NN correlations are taken into account, the value of $N_{(10)}$ is practically unchanged, whereas the

number of pairs in the (01) state is decreased in favor of the state (11). The reason for that was nicely explained in Refs. [23,40]: It is attributable to some kind of many-body effects induced by tensor correlations between particles "2" and "3," generating a spin flip of particle "2" and giving rise to the state (11) between particles "2" and "1." These effects are automatically included in our calculations, because "exact" wave functions are used in case of few-nucleon systems and a cluster expansion embodying many-body clusters is adopted in our approach for complex nuclei.

B. The spin-isospin contributions to the momentum distributions

We apply here Eq. (26) (with $\mathbf{k}_1 \equiv \mathbf{k}$), obtaining for the proton momentum distributions in ^3He

$$n_3^p(\mathbf{k}) = \frac{3}{8}n_{T=0}^{(pn)}(\mathbf{k}) + \frac{5}{8}n_{T=1}(\mathbf{k}) \quad (60)$$

$$= n_3^{p(10)}(\mathbf{k}) + n_3^{p(00)}(\mathbf{k}) + n_3^{p(01)}(\mathbf{k}) + n_3^{p(11)}(\mathbf{k}), \quad (61)$$

because there is only one pp and one pn pair containing proton "1," whereas the neutron distribution is given by

$$n_3^n(\mathbf{k}) = \frac{3}{4}n_{T=0}^{(pn)}(\mathbf{k}) + \frac{1}{4}n_{T=1}(\mathbf{k}) \quad (62)$$

$$= n_3^{n(10)}(\mathbf{k}) + n_3^{n(00)}(\mathbf{k}) + n_3^{n(01)}(\mathbf{k}) + n_3^{n(11)}(\mathbf{k}), \quad (63)$$

because there are two pn pairs containing neutron "1" and no pp pairs. The momentum distributions of ^4He , ^{16}O , and ^{40}Ca are given, respectively, by

$$n_4(\mathbf{k}) = \frac{1}{2}n_{T=0}^{(pn)}(\mathbf{k}) + \frac{1}{2}n_{T=1}(\mathbf{k}) \quad (64)$$

$$= n_4^{(10)}(\mathbf{k}) + n_4^{(00)}(\mathbf{k}) + n_4^{(01)}(\mathbf{k}) + n_4^{(11)}(\mathbf{k}), \quad (65)$$

$$n_{16}(\mathbf{k}_1) = \frac{3}{10}n_{T=0}^{(pn)}(\mathbf{k}) + \frac{7}{10}n_{T=1}(\mathbf{k}) \quad (66)$$

$$= n_{16}^{(10)}(\mathbf{k}) + n_{16}^{(00)}(\mathbf{k}) + n_{16}^{(01)}(\mathbf{k}) + n_{16}^{(11)}(\mathbf{k}), \quad (67)$$

$$n_{40}(\mathbf{k}) = \frac{7}{25}n_{T=0}^{(pn)}(\mathbf{k}) + \frac{19}{25}n_{T=1}(\mathbf{k}) \quad (68)$$

$$= n_{40}^{(10)}(\mathbf{k}) + n_{40}^{(00)}(\mathbf{k}) + n_{40}^{(01)}(\mathbf{k}) + n_{40}^{(11)}(\mathbf{k}), \quad (69)$$

where Eqs. (22) and (23) have been used,

$$n_{T=1}^{(pn)}(\mathbf{k}) = n_{T=1}^{(pp)}(\mathbf{k}) \equiv n_{T=1}(\mathbf{k}), \quad (70)$$

and

$$\int n_A(\mathbf{k}) d\mathbf{k} = \int n_{T=0}^{pn}(\mathbf{k}) d\mathbf{k} = \int n_{T=1}(\mathbf{k}) d\mathbf{k} = 1. \quad (71)$$

The results of calculations of the spin-isospin contributions to the momentum distribution of ^3He , ^4He , ^{16}O , and ^{40}Ca , are presented in Figs. 11–15. The following remarks are in order: (i) the contribution from the (00) state is negligible in both few-nucleon systems and complex nuclei; (ii) the (11) state in ^3He and ^4He is small, both at low and large values of k , but it plays a relevant role in the region $1.5 \lesssim k \lesssim 3 \text{ fm}^{-1}$; (iii) in the proton distribution of ^3He (Fig. 11) the (01) contribution is important everywhere except in the region $1.5 \lesssim k \lesssim 3 \text{ fm}^{-1}$,

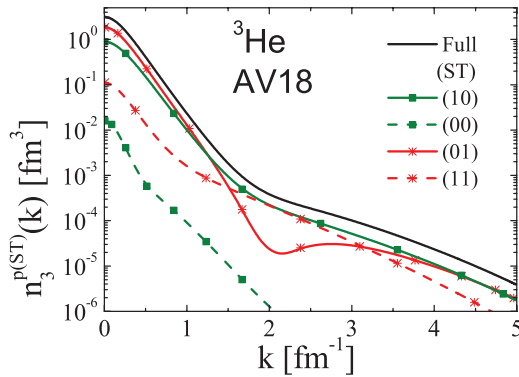


FIG. 11. (Color online) The various spin-isospin contributions (ST) to the proton momentum distribution of ${}^3\text{He}$. Wave function from Ref. [26], AV18 interaction. The continuous line without symbols is the sum of the four contributions [cf. Eq. (61)].

whereas in the neutron distributions (Fig. 12), thanks to the different weight of the (01) state [1/4 instead of 5/8; cf. Eqs. (60) and (62)], the contribution from this state is much smaller; (iv) in complex nuclei the (11) state (odd relative orbital momenta) plays a dominant role, both in the independent particle model and in the many-body approach (cf. Table III and Figs. 14 and 15). Thus, in summary, we found that all spin-isospin components, except the (00) one, contribute to the high-momentum content of the momentum distributions and only in the case of the neutron distribution in the nonisoscalar nucleus ${}^3\text{He}$, the deuteronlike state (10) is the dominant contribution.

To provide further evidence of the A independence of SRC, we show in Fig. 16 the “elementary” quantities $n_{T=0}^{(pn)}(\mathbf{k}_1)$ and $n_{T=1}(\mathbf{k}_1)$ for different nuclei, and it can be seen that, starting from $k \equiv |\mathbf{k}_1| \simeq 2 \text{ fm}^{-1}$, they follow the same pattern.

V. THE MOMENTUM DISTRIBUTIONS OF NUCLEI VS THE DEUTERON MOMENTUM DISTRIBUTION

As it clearly appears in Fig. 6, at $k \gtrsim 1.5\text{--}2 \text{ fm}^{-1}$ the momentum distribution of nuclei exhibits a trend similar to

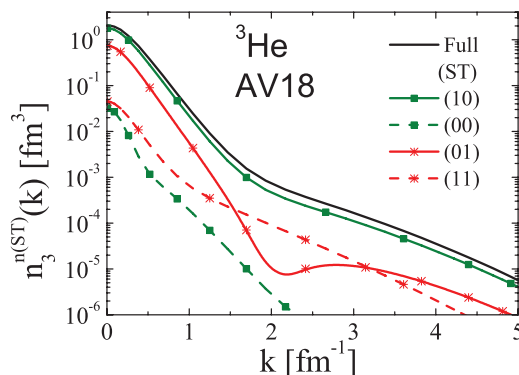


FIG. 12. (Color online) The same as in Fig. 11 but for the neutron distribution [cf. Eq. (63)].

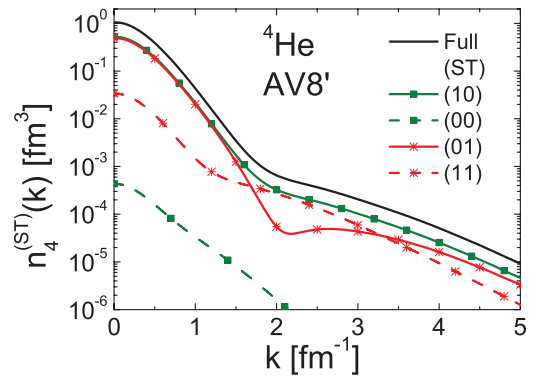


FIG. 13. (Color online) The various spin-isospin contributions to the proton momentum distribution of ${}^4\text{He}$ [cf. Eq. (65)]. Wave function from Ref. [25], AV8' interaction.

the one of the deuteron.² However, a quantitative analysis of the ratio

$$R_{A/D}(k) = \frac{n_A(k)}{n_D(k)} \quad (72)$$

is in order, because $n_A(k)$ is usually interpreted as the scaled deuteron momentum distribution, i.e., $R_{A/D}(k) = n_A(k)/n_D(k) \simeq \text{const}$. Such an interpretation originated long ago either from the use of pioneering theoretical many-body calculations [17–20] or by assuming it as an input for the calculations of $n_A(k_1)$ at $k \geq k_F$ [21] when variational Monte Carlo calculations were difficult to perform at high values of the momentum, or by obtaining the momentum distributions from an average value of the pn and pp spectral functions [12]. Having nowadays at disposal advanced many-body calculations of the momentum distributions performed with realistic models of the two-nucleon interactions, a quantitative analysis of Eq. (72) is timing. To this end, we show in Fig. 17 the ratio $R_{A/D}(k)$ calculated with realistic many-body wave functions. It clearly appears that starting from $k \gtrsim 2 \text{ fm}^{-1}$, the ratio is not a constant but appreciably increases with k .

²In the rest of the paper we frequently use the notation ${}^2\text{H} \equiv D$.

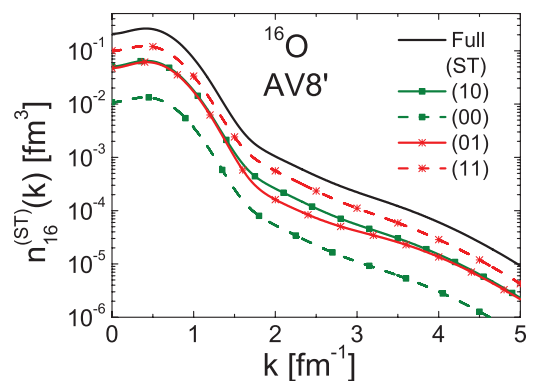


FIG. 14. (Color online) The various spin-isospin contributions to the momentum distribution of ${}^{16}\text{O}$ [cf. Eq. (67)]. Wave function from Ref. [31], AV8' interaction.

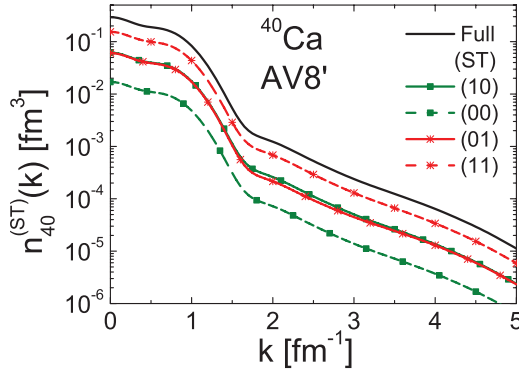


FIG. 15. (Color online) The same as in Fig. 14, but for ^{40}Ca [cf. Eq. (69)].

Let us discuss the origin of such an increase. A first possible origin should be sought in the different role played by pn and pp correlations. As a matter of fact, the proton and neutron momentum distributions in ^3He shown in Fig. 18 exhibit a different rate of increase, which can qualitatively be understood in terms of SRCs as follows: In ^3He the proton momentum distribution is affected by SRCs acting in one pn and one pp pairs, in the former pair the deuteronlike state (10) is three times larger than the (01) state, whereas in the latter pair the deuteronlike state is totally missing; on the contrary, the neutron distribution is affected by SRCs acting in two proton-neutron pairs, with a pronounced dominance of the deuteronlike state (10); therefore, one expects that around $k \simeq 2 \text{ fm}^{-1}$, where, np SRCs dominate over pp SRC [10,21], $n_3^n/n_D \simeq 2$ and $n_3^p/n_D \simeq 1$, which indeed seems to be the case. However, other effects of different origin can contribute to the deviation of the ratio $n_A(k)/n_D(k)$ from a constant. These are attributable to the c.m. motion of a pn pair in a nucleus, to the different role played by the states (01) and (11) in different nuclei, and, particularly, to the fact that, being the one-nucleon momentum distribution the integral of the two-body distribution over k_2 , $n_A(\mathbf{k}_1) = \int n_A(\mathbf{k}_1, \mathbf{k}_2) d\mathbf{k}_2$, it may contain configurations different from the deuteron one (back-to-back nucleons). To better investigate

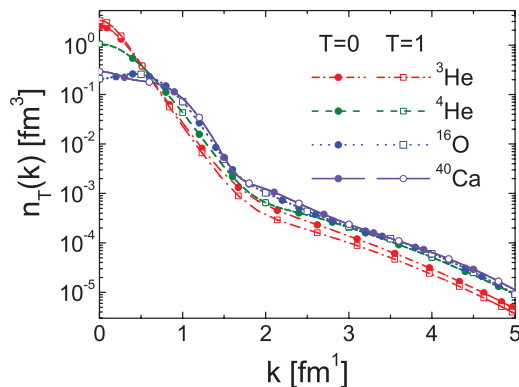


FIG. 16. (Color online) The isospin $T = 0$ and $T = 1$ contributions to the proton momentum distributions [Eqs. (22) and (23)].

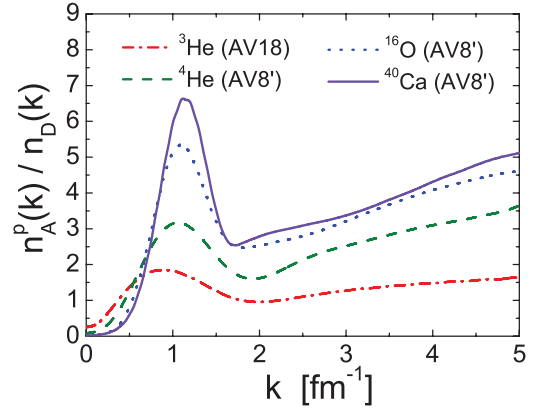


FIG. 17. (Color online) The ratio of the proton momentum distribution of nucleus A shown in the previous figures to the deuteron momentum distributions.

these possibilities, let us consider the spin-isospin ratio

$$R_{A/D}^{(ST)}(k) = \frac{n_A^{(ST)}(k)}{n_D(k)}, \quad (73)$$

which is shown in Figs. 19–23 (note that, as stressed in the caption of the figures, the quantity $n_A^{(ST)}$ includes the proper coefficients which multiply the “elementary” quantities $n_T^{N_1 N_2}$). It can be seen that the behavior of the proton and neutron ratios for ^3He clearly shows that in the region $1.5 \lesssim k \lesssim 3 \text{ fm}^{-1}$ the former is governed by the (01) state in the pp and pn pairs; on the contrary, the neutron ratio is fully dominated by the deuteronlike (10) state in the two pn pairs. The most interesting ratio is $R_{A/D}^{(10)}(k) = n_A^{(10)}(k)/n_D(k)$, because it provides information on the behavior of the deuteronlike pairs in nuclei; it can be seen that in the region of SRCs ($k \gtrsim 2 \text{ fm}^{-1}$) $R_{A/D}^{(10)}$ increases with increasing value of k , with a different rate of increase for different nuclei: it is about 30% in the neutron momentum distribution of ^3He , and of the order of 100% in other nuclei. As already pointed out, the increase of the ratio $R_{A/D}^{(ST)}(k)$ with k could also be attributable to the c.m. motion of the pair in the nucleus. To take this into account

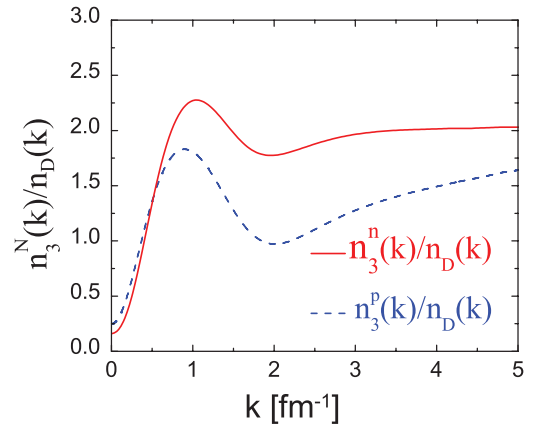


FIG. 18. (Color online) The ratio of the neutron, $n_3^n(k)$, and proton, $n_3^p(k)$, distributions in ^3He to the deuteron momentum distributions, $n_D(k)$.

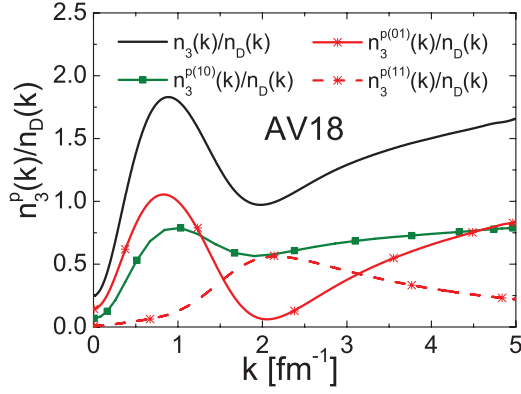


FIG. 19. (Color online) The various spin-isospin contributions to the ratio of the proton momentum distributions of ${}^3\text{He}$ [Eq. (61)] to the deuteron momentum distributions. Wave function from Ref. [26], AV18 interaction.

is no easy task. As a matter of fact, consider the simple case when the (10) two-body momentum distribution factorizes in the following form Ref. [12]:

$$n_{(10)}^{pn}(\mathbf{k}_1, \mathbf{k}_2) = n_{10}^{pn}(\mathbf{k}_{\text{rel}}, \mathbf{K}_{\text{c.m.}}) = n_{10}^{pn}(k_{\text{rel}}, K_{\text{c.m.}}, \theta) \simeq n_D(k_{\text{rel}}) n_{\text{c.m.}}^A(K_{\text{c.m.}}), \quad (74)$$

where $n_{\text{c.m.}}(K_{\text{c.m.}})$, calculated from a many-body approach in Ref. [11], can be approximated by a $0S$ wave function. In Refs. [11,48], Eq. (74) has indeed been shown to hold, but only in a restricted region of k_{rel} and $K_{\text{c.m.}}$, namely

$$K_{\text{c.m.}} \lesssim 1.0 - 2.0 \text{ fm}^{-1}, \quad k_{\text{rel}} \gtrsim k_{\text{rel}}^- = f_A(K_{\text{c.m.}}), \quad (75)$$

where the function f_A depends upon $K_{\text{c.m.}}$ and A in such a way that the value of k_{rel}^- increases with increasing values of $K_{\text{c.m.}}$. Thanks to momentum conservation $\mathbf{k}_2 = -(\mathbf{k}_1 + \mathbf{K}_{\text{c.m.}})$, one can write

$$n_{(10)}^{pn}(k_1) \simeq \int n_D \left(\left| \mathbf{k}_1 - \frac{\mathbf{K}_{\text{c.m.}}}{2} \right| \right) n_{\text{c.m.}}(|\mathbf{K}_{\text{c.m.}}|) d\mathbf{K}_{\text{c.m.}} \quad (76)$$

which shows that only in the case of a pn pair at rest, i.e., $n_{\text{c.m.}}(\mathbf{K}_{\text{c.m.}}) = \delta(\mathbf{K}_{\text{c.m.}})$, one has $n_{(10)}^{pn}(k_1) \simeq n_D(k_1)$ $R_{A/D}^{(ST)}(k_1) \simeq \text{const}$. The convolution of the deuteron momentum distributions with the c.m. motion leads to an increase of

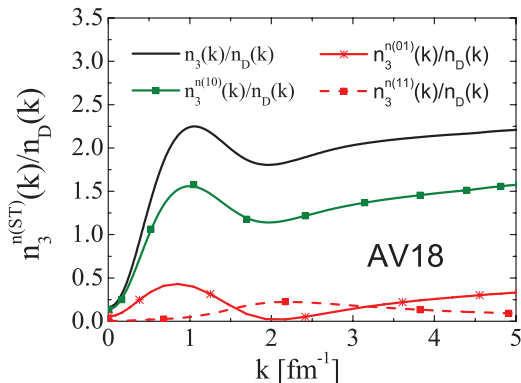


FIG. 20. (Color online) The same as in Fig. 19, but for the neutron distribution.

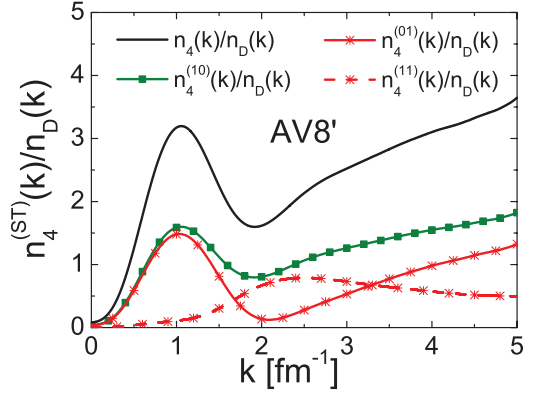


FIG. 21. (Color online) The various spin-isospin contributions to the ratio of the proton momentum distributions of ${}^4\text{He}$ to the deuteron momentum distributions. Wave function from Ref. [26], AV8' interaction.

$n_{10}^{pn}(k_1)$, whose magnitude and rate of increase depend upon the detailed forms of $n_{10}^{pn}(k_{\text{rel}})$ and $n_{\text{c.m.}}(K_{\text{c.m.}})$; moreover, because, as already stressed, the one-body momentum distribution is the integral of the two-body momentum distribution, configurations different from the factorized one [Eq. (74)] can contribute to the integral [Eq. (76)].

A. On the short-range deuteronlike configurations in nuclei

A particular useful quantity to understand SRC in nuclei is the one that is obtained by integrating the two-nucleon momentum distribution of the state (10) in a narrow range of the c.m. momentum ($K_{\text{c.m.}} \lesssim 1 - 1.5 \text{ fm}^{-1}$), when the c.m. and relative motions are decoupled, and Eq. (74) is satisfied [11], namely,

$$n_{D/A}^{pn}(k_{\text{rel}}) = \int n_{(10)}^{pn}(k_{\text{rel}}, K_{\text{c.m.}}, \theta) d\mathbf{K}_{\text{c.m.}} \simeq n_D(k_{\text{rel}}) 4\pi \int_0^{K_{\text{c.m.}}^+} n_{\text{c.m.}}^A(K_{\text{c.m.}}) K_{\text{c.m.}}^2 dK_{\text{c.m.}} \quad (77)$$

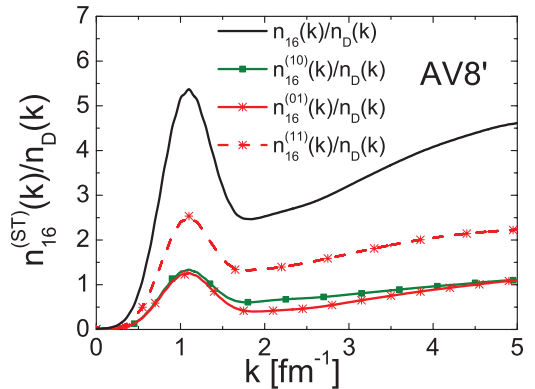


FIG. 22. (Color online) The various spin-isospin contributions to the ratio of the momentum distribution of ${}^{16}\text{O}$ to the deuteron momentum distributions. Wave function from Ref. [31], AV8' interaction.

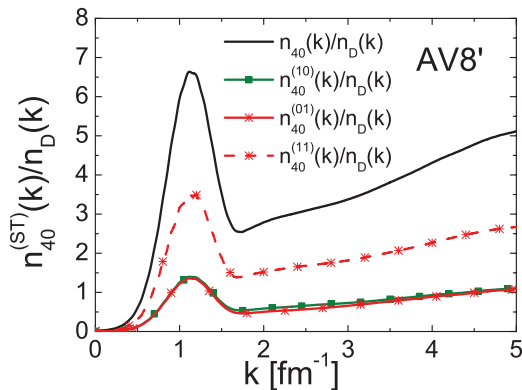


FIG. 23. (Color online) The various spin-isospin contributions to the ratio of the momentum distribution of ^{40}Ca to the deuteron momentum distributions. Wave function from Ref. [31], AV8' interaction.

In Ref. [3] the $2N$ SRC probability in the deuteron has been defined as the integral of the deuteron momentum distribution in the range $k_{\text{rel}} \gtrsim 1.5 \text{ fm}^{-1}$ (cf. Table IV); therefore, we can consider as the analog in a nucleus the quantity

$$\mathcal{P}_{D/A} = 4\pi \int_{1.5}^{\infty} n_{D/A}^{pn}(k_{\text{rel}}) k_{\text{rel}}^2 dk_{\text{rel}}, \quad (78)$$

where $n_{D/A}^{pn}$ is given by Eq. (77). We can also define the total number of quasideuteron short-range correlated pairs as follows:

$$N_{D/A} = N_{(10)}^A \mathcal{P}_{D/A}, \quad (79)$$

where the number of $N_{(10)}^A$ pairs is listed in Table III. The calculated values of the partial probability $\mathcal{P}^{N_1} = 4\pi \int_{1.5}^{\infty} [n_0(k) + n_1(k)] k^2 dk$ [Eq. (45)], predicted by different NN interactions, is shown in Table IV, and the quantities $\mathcal{P}_{D/A}$ and $N_{D/A}$ are given in Table V. Because \mathcal{P}^{N_1} includes all spin-isospin components and momentum configurations, whereas only deuteronlike configurations [(ST) = (10) and $\mathbf{k}_1 = -\mathbf{k}_1$] are included in $\mathcal{P}_{D/A}$, our result $\mathcal{P}_{D/A} < \mathcal{P}^{N_1}$ is fully justified. Moreover, the decreasing behavior of $\mathcal{P}_{D/A}$ with A can easily be understood as owing to the increasing importance of higher c.m. momentum components of the pair, resulting in flatter c.m. distributions in heavier nuclei (cf., Fig. 24), so that only a smaller part of the distribution is included in the

TABLE IV. The value of the $2N$ SRCs partial probability [Eq. (45)] in the deuteron, $4\pi \int_{1.5}^{\infty} n_D(k) k^2 dk$, and in complex nuclei $4\pi \int_{1.5}^{\infty} [n_0(k) + n_1(k)] k^2 dk$ (cf. Table II) obtained with momentum distribution resulting from many-body calculations performed with different NN interactions. The result (CS) of the phenomenological model of Ref. [12] is also shown.

NN interaction	^2H	$^3\text{He}(n)$	$^3\text{He}(p)$	^4He	^{16}O	^{40}Ca
RSC	0.04	—	—	0.09	0.12	—
AV14	0.036	—	—	0.11	0.14	—
AV8'	0.036	—	—	0.09	0.10	0.10
AV18	0.037	0.067	0.041	—	—	—
CS	0.033	0.079	0.046	0.09	0.10	0.14

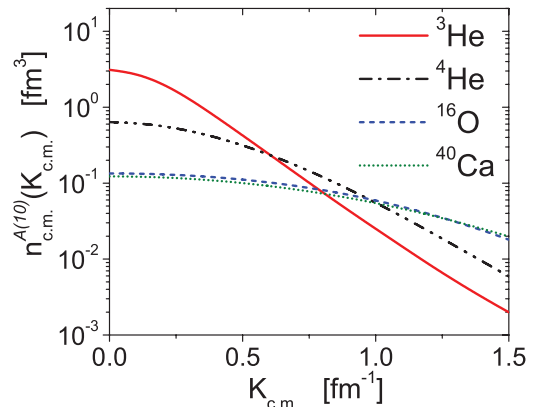


FIG. 24. (Color online) The c.m. momentum distribution in the state (10) $n_{c.m.}^{A(10)}(K_{c.m.})$ in ^3He , ^4He , ^{16}O , and ^{40}Ca .

integral over $K_{c.m.}$. We have also considered the quantity $a_{D/A}$, the per-nucleon probability of deuteronlike configurations in A with respect to the probability of SRCs in the deuteron ($\simeq 0.04$). Our values for $A < 40$ are less than the values of a_2 extracted from the $A(e, e')X$ experiments [3–5]; however, such a comparison is a premature one, because, from one side, nondeuteronlike configurations which occur outside the factorization region should be considered in the theoretical calculation (e.g., the c.m. motion of the pair [5,46]) and, from the other side, a careful investigation of the effects of FSI on the extraction of a_2 from the inclusive $A(e, e')X$ cross-section ratio should also be considered. We should also mention, in this respect, that the values of a_2 were also recently calculated in Ref. [46] within an approach in which only $L = 0$ pairs prone to SRCs were considered (cf. Table III), obtaining results that coincide with the ones obtained in the present paper for $A = 3, 4$, and which are lower for $A > 4$.

VI. SUMMARY AND CONCLUSIONS

Recently, several A -independent features of SRCs in few-nucleon systems (^2H , ^3H , ^3He , and ^4He) have been demonstrated by calculating the dependence of two-body momentum distributions upon the relative momentum $|\mathbf{k}_{\text{rel}}| \equiv k_{\text{rel}}$ of the correlated pair [23], as well as upon the c.m. momentum $|\mathbf{K}_{c.m.}| \equiv K_{c.m.}$ and the angle between $\mathbf{K}_{c.m.}$ and \mathbf{k}_{rel} [11]. These calculations have been performed with exact wave functions resulting from the solution of the nonrelativistic Schrödinger equation, using modern bare NN interactions, featuring strong short-range repulsion and intermediate-range tensor attraction, e.g., the Argonne-Urbana models.

In the present paper, using the same many-body approach and interactions, we have addressed the problem of the effects of SRCs, and their spin-isospin components, on the one-nucleon momentum distributions $n_A(k)$ of few-nucleon systems and complex nuclei. The momentum distribution, besides being *per se* a relevant quantity in nuclear theory, plays a relevant role in the interpretation of various experimental data, in particular in inclusive experiments of lepton scattering off nuclei at medium and high energies.

TABLE V. The values of $\mathcal{P}_{D/A}$ [Eq. (78)] and $N_{D/A}$ [Eq. (79)] calculated in correspondence of $K_{\text{c.m.}}^+ = 1.5 \text{ fm}^{-1}$. The quantity $a_{D/A} = [(2/A)][N_{D/A}/N_{D/D}]$ is the per-nucleon probability of deuteronlike $[(ST) = (10)]$ 2N SRC in A with respect to the deuteron.

$K_{\text{c.m.}}^+$ (fm $^{-1}$)	${}^2\text{H}$			${}^3\text{He}$			${}^4\text{He}$			${}^{16}\text{O}$			${}^{40}\text{Ca}$		
	$\mathcal{P}_{D/A}$	$N_{D/A}$	$a_{D/A}$												
1.5	0.04	0.04	1	0.04	0.06	1	0.04	0.12	1.5	0.031	0.93	2.9	0.030	4.9	6.1

Using the proper diagonal and nondiagonal one- and two-body spin- and isospin- dependent density matrices, we have derived in Sec. II the expression of the momentum distributions of a nucleon belonging to a NN pair in a state with total spin S and isospin T . In Sec. III we have presented some general concepts concerning nucleon momentum distributions and a clear-cut way to separate them in mean-field and SRC contributions, and have analyzed the results of the most recent calculations of the momentum distributions for nuclei with $A = 2, 3, 4, 16$, and 40 , performed within realistic many-body approaches and modern NN interactions. The aim was to ascertain whether some general features of the momentum distributions could be established within the solution of the nuclear many-body problem, in terms of realistic bare NN interactions.

The results of our analysis have shown indeed that, even if quantitative differences are provided by different interactions and many-body approaches, the following general features of the momentum distributions can be singled out, namely: (i) at $k \lesssim 1\text{--}1.5 \text{ fm}^{-1}$, the mean-field approach dominates the distributions, with a resulting sizeable A dependence; (ii) at larger values of k , of the order of 2 fm^{-1} , owing to the effects of SRCs, the momentum distributions abruptly change their slope, and, apart from an A -dependent scaling factor, exhibit a k dependence which is very similar in different nuclei; (iii) the correlated part of the momentum distribution is by orders of magnitude larger than the predictions of any mean-field approach, so that experiments providing even rough information on high-momentum components would be able to rule out mean-field predictions.

Similar conclusions, reached in the past by phenomenological calculations (see, e.g., Refs. [12,15]), are therefore quantitatively confirmed by the present systematic analysis. After having checked that the evaluation of the high-momentum part of $n_A(k)$ is well under control, we turned in Sec. IV to the calculation of the spin-isospin structure of the momentum distributions. First of all, we calculated the number of NN pairs in various spin-isospin states in different nuclei, both within the independent particle models and in many-body approaches embodying SRCs, finding agreement with calculations performed by different groups, confirming that SRCs have very small effects on the number of isosinglet pairs in state (10), unlike what happens with isotriplet pairs in state (01), whose number is decreased in favor of the pairs in (11) state.

We have calculated the contribution of the states $(ST) = (10), (00), (01)$, and (11) to the momentum distributions, finding that all of them, except the state (00), have comparable effects in a wide range of momentum. The contribution of

the isosinglet state $T = 0$ is almost entirely exhausted by the (10) state, whereas both states (01) and (11) contribute to the isotriplet state $T = 1$. We found that at momentum values $k \gtrsim 2 \text{ fm}^{-1}$, the contribution of both isosinglet and isotriplet states follow the same pattern, independently of A , which represents further evidence of the general scaling behavior of SRCs.

A systematic and quantitative comparison of $n_A(k)$, and its spin-isospin components $n_A^{ST}(k)$, with the deuteron momentum distribution $n_D(k)$, has been presented in Sec. IV, by analyzing the ratios $n_A^{ST}(k)/n_D(k)$. We found that in the region of SRCs, $k \gtrsim 2 \text{ fm}^{-1}$, this ratio does not stay constant but increases with increasing k , and interpreted such a behavior as owing to the presence in the momentum distribution of two-nucleon momentum configurations arising from the c.m. motion of a pair and differing from the back-to-back nucleons configuration. Our spin-isospin dependent approach allowed us to calculate also (i) the relative momentum distribution of a proton-neutron pair moving with small c.m. momentum and its integral in the range $1.5 < k < \infty$, a quantity which is assumed to represent the probability of two-nucleon SRCs in a nucleus, finding similar values ($\simeq 0.04$) in a wide range of A , namely $2 \leq A \leq 40$; (ii) the total number of SRCs pairs in (10) state, interpreting its A dependence in terms of the A dependence of the c.m. momentum distribution; (iii) the per-nucleon probability of deuteronlike SRCs in nuclei, a quantity which is under active experimental investigation.

In closing this paper, we would like to stress that the properties of SRCs we have found depend obviously upon the wave function we have used to calculate the density matrices and momentum distributions. In case of $A = 2, 3$, and 4 systems the ground-state wave functions represent the *ab initio* solution of the many-body nonrelativistic Schrödinger equation given in terms of modern bare NN interactions, whereas, in the case of complex nuclei, they represent the variational solution of the same equation. The high-momentum content of the ground-state wave function will obviously depend upon the used NN interaction. In this respect it should be recalled that phase shift data characterizing elastic on-shell NN scattering do not determine uniquely the details of the short-range interaction; moreover, in a many-body bound nuclear systems, two interacting nucleons that experience interaction with surrounding nucleons are off shell; i.e., their energy is not related to their relative momentum, with the resulting complication that the off-shell behavior of the interaction cannot be determined uniquely from elastic phase shifts.

As a result, a family of different phase-equivalent potentials can be derived (see, e.g., [39,49–51]), producing different

high-momentum contents of the many-body nuclear wave functions. This fact points to the importance of the investigation of the high momentum part of the nucleon momentum distributions (see, e.g., [52]). At the same time, it should also be stressed that the interaction we have used (e.g., the AV18 or/and AV $8'$ ones) are currently being used in that class of successful *ab initio* many-body calculations (e.g., the Unitary Correlation Operator Method (UCOM) [30] and the no-core shell model approach [53]) where various renormalization group (RG) methods [54] are used to soften the short-range and tensor interactions of the original bare interaction, so as to improve the convergence of the diagonalization of the many-body Hamiltonian. As a result, the finally evolved ground-state wave function exhibits a low degree of SRCs.

It would appear that these methods are in conflict with the traditional direct solution of the many-body Schrödinger equation with bare NN interaction, producing ground-state wave functions containing a large degree of SRCs, arising from the strong short-range repulsive and the intermediate-range

attractive tensor forces. This, however, is not the case, as discussed in two recent papers [55,56] (see also Ref. [23]), stressing the necessity to evolve, together with the NN interaction, also the momentum distribution operator.

Preliminary results for the two-body system [55], and Fermi and electron gases [56], show indeed that the high-momentum content of the momentum distributions, and their scaling behavior stressed in the present and many other papers can also be predicted within low-momentum effective theories.

ACKNOWLEDGMENTS

We thank the Pisa group for providing us with the code for the calculation of deuteron momentum distributions and the three-nucleon wave function. H.M. is grateful to INFN, Sezione di Perugia for warm hospitality. We thank CASPUR for Grant No. SRCnuc3 - Short-Range Correlations in Nuclei, within the Standard HPC Grants 2012 program.

-
- [1] A. Tang, J. W. Watson, J. L. S. Aclander, J. Alster, G. Asryan *et al.*, *Phys. Rev. Lett.* **90**, 042301 (2003).
- [2] R. Shneor *et al.* (Jefferson Lab Hall A Collaboration), *Phys. Rev. Lett.* **99**, 072501 (2007).
- [3] K. S. Egiyan *et al.* (CLAS Collaboration), *Phys. Rev. Lett.* **96**, 082501 (2006).
- [4] L. L. Frankfurt, M. I. Strikman, D. B. Day, and M. Sargsyan, *Phys. Rev. C* **48**, 2451 (1993).
- [5] N. Fomin, J. Arrington, R. Asaturyan, F. Benmokhtar, W. Boeglin *et al.*, *Phys. Rev. Lett.* **108**, 092502 (2012).
- [6] R. Subedi, R. Shneor, P. Monaghan, B. D. Anderson, K. Aniol *et al.*, *Science* **320**, 1476 (2008).
- [7] L. L. Frankfurt and M. I. Strikman, *Phys. Rep.* **76**, 215 (1981).
- [8] M. M. Sargsian, T. V. Abrahamyan, M. I. Strikman, and L. L. Frankfurt, *Phys. Rev. C* **71**, 044615 (2005).
- [9] R. Schiavilla, R. B. Wiringa, S. C. Pieper, and J. Carlson, *Phys. Rev. Lett.* **98**, 132501 (2007).
- [10] M. Alvioli, C. Ciofi degli Atti, and H. Morita, *Phys. Rev. Lett.* **100**, 162503 (2008).
- [11] M. Alvioli, C. Ciofi degli Atti, L. P. Kaptari, C. B. Mezzetti, H. Morita, and S. Scopetta, *Phys. Rev. C* **85**, 021001 (2012).
- [12] C. Ciofi degli Atti and S. Simula, *Phys. Rev. C* **53**, 1689 (1996).
- [13] J. Arrington, D. W. Higinbotham, G. Rosner, and M. Sargsian, *Prog. Part. Nucl. Phys.* **67**, 898 (2012).
- [14] L. Frankfurt, M. Sargsian, and M. Strikman, *Int. J. Mod. Phys. A* **23**, 2991 (2008).
- [15] M. Dal Ri, O. Bohigas, and S. Stringari, *Nucl. Phys. A* **376**, 81 (1982).
- [16] C. Ciofi degli Atti, E. Pace, and G. Salme, *Phys. Rev. C* **43**, 1155 (1991).
- [17] J. G. Zabolitzky and W. Ey, *Phys. Lett.* **76B**, 527 (1978).
- [18] J. W. Van Orden, W. Truex, and M. K. Banerjee, *Phys. Rev. C* **21**, 2628 (1980).
- [19] O. Benhar, C. Ciofi degli Atti, S. Liuti, and G. Salmè, *Phys. Lett. B* **177**, 135 (1986).
- [20] X.-D. Ji and J. Engel, *Phys. Rev. C* **40**, 497 (1989).
- [21] R. Schiavilla, V. R. Pandharipande, and R. B. Wiringa, *Nucl. Phys. A* **449**, 219 (1986).
- [22] S. C. Pieper, R. B. Wiringa, and V. R. Pandharipande, *Phys. Rev. C* **46**, 1741 (1992).
- [23] H. Feldmeier, W. Horiuchi, T. Neff, and Y. Suzuki, *Phys. Rev. C* **84**, 054003 (2011).
- [24] H. Morita, Y. Akaishi, and H. Tanaka, *Prog. Theor. Phys.* **79**, 863 (1988).
- [25] H. Morita *et al.* (to be published).
- [26] A. Kievsky, S. Rosati, and M. Viviani, *Nucl. Phys. A* **551**, 241 (1993).
- [27] W. Gloeckle, H. Witala, D. Huber, H. Kamada, and J. Golak, *Phys. Rep.* **274**, 107 (1996).
- [28] F. Arias de Saavedra, C. Bisconti, G. Co', and A. Fabrocini, *Phys. Rep.* **450**, 1 (2007).
- [29] S. C. Pieper and R. B. Wiringa, *Annu. Rev. Nucl. Part. Sci.* **51**, 53 (2001).
- [30] R. Roth, T. Neff, and H. Feldmeier, *Prog. Part. Nucl. Phys.* **65**, 50 (2010).
- [31] M. Alvioli, C. Ciofi degli Atti, and H. Morita, *Phys. Rev. C* **72**, 054310 (2005).
- [32] K. Varga and Y. Suzuki, *Phys. Rev. C* **52**, 2885 (1995).
- [33] Y. Suzuki, W. Horiuchi, M. Orabi, and K. Arai, *Few-Body Syst.* **42**, 33 (2008).
- [34] Y. Suzuki and W. Horiuchi, *Nucl. Phys. A* **818**, 188 (2009).
- [35] R. V. Reid, *Ann. Phys. (NY)* **50**, 411 (1968).
- [36] M. Lacombe, B. Loiseau, J. M. Richard, R. VinhMau, J. Conte, P. Pires, and R. deTourreil, *Phys. Rev. C* **21**, 861 (1980).
- [37] B. S. Pudliner, V. R. Pandharipande, J. Carlson, S. C. Pieper, and, R. B. Wiringa, *Phys. Rev. C* **56**, 1720 (1997).
- [38] R. B. Wiringa, R. A. Smith, and T. A. Ainsworth, *Phys. Rev. C* **29**, 1207 (1984).
- [39] R. B. Wiringa, V. G. J. Stoks, and R. Schiavilla, *Phys. Rev. C* **51**, 38 (1995).
- [40] J. L. Forest, V. R. Pandharipande, S. C. Pieper, R. B. Wiringa, R. Schiavilla, and A. Arriaga, *Phys. Rev. C* **54**, 646 (1996).
- [41] C. Ciofi degli Atti, E. Pace, and G. Salmè, *Phys. Lett. B* **141**, 14 (1984).
- [42] C. Ciofi degli Atti and S. Liuti, *Phys. Lett. B* **225**, 215 (1989).

- [43] F. Benmokhtar *et al.* (Jefferson Lab Hall A Collaboration), *Phys. Rev. Lett.* **94**, 082305 (2005).
- [44] J. F. J. van den Brand, H. P. Blok, R. Ent, E. Jans, G. J. Kramer, J. B. J. M. Lanen, L. Lapikas, E. N. M. Quint, G. van der Steenhoven, and P. K. A. de Witt Huberts, *Phys. Rev. Lett.* **60**, 2006 (1988); A. Magnon *et al.*, *Phys. Lett. B* **222**, 352 (1989).
- [45] R. B. Wiringa, *Phys. Rev. C* **73**, 034317 (2006).
- [46] M. Vanhalst, W. Cosyn, and J. Ryckebusch, *Phys. Rev. C* **84**, 031302 (2011).
- [47] M. Vanhalst, J. Ryckebusch, and W. Cosyn, *Phys. Rev. C* **86**, 044619 (2012).
- [48] C. Ciofi degli Atti, L. P. Kaptari, H. Morita, and S. Scopetta, *Few-Body Syst.* **50**, 243 (2011).
- [49] R. Machleidt, *Phys. Rev. C* **63**, 024001 (2001).
- [50] E. Epelbaum, W. Glöckle, and U.-G. Meissner, *Nucl. Phys. A* **747**, 362 (2005).
- [51] W. N. Polizou and W. Glöckle, *Few-Body Syst.* **9**, 97 (1990).
- [52] J. P. Vary, *Phys. Rev. C* **7**, 521 (1973).
- [53] P. Navrátil, S. Quaglioni, I. Stetcu, and B. Barrett, *J. Phys. G* **36**, 083101 (2009); P. Maris, J. P. Vary, and A. M. Shirokov, *Phys. Rev. C* **79**, 014308 (2009).
- [54] S. K. Bogner, R. J. Furnstahl, and A. Schwenk, *Prog. Part. Nucl. Phys.* **65**, 94 (2010).
- [55] E. R. Anderson, S. K. Bogner, R. J. Furnstahl, and R. J. Perry, *Phys. Rev. C* **82**, 054001 (2010).
- [56] S. K. Bogner and D. Roscher, *Phys. Rev. C* **86**, 064304 (2012).